Comparative study for the calculation of the Lyapunov spectrum from nonlinear experimental signals

Antonis Karantonis and Michael Pagitsas
Laboratory of Physical Chemistry, Department of Chemistry, Aristotle University of Thessaloniki, 54006 Thessaloniki, Greece
(Received 28 June 1995)

A uniform formalism is introduced for the description and comparison of the algorithms of Sano and Sawada [M. Sano and Y. Sawada, Phys. Rev. Lett. **55**, 1082 (1985)] and Eckmann *et al.* [J.-P. Eckmann, S. O. Kamphorst, D. Ruelle, and S. Cilibert, Phys. Rev. A **34**, 4971 (1986)], for the calculation of the Lyapunov spectrum from experimental data. It is shown that both algorithms coincide for the calculation of the maximum Lyapunov exponent and differ for the other exponents. A numerical application is carried out which confirms the above result. A detailed investigation of the dependence of the Sano and Sawada and the Eckmann *et al.* algorithms on the parameters of the algorithms, the signal and the reconstruction of the attractor, for the calculation of the whole Lyapunov spectrum is presented. Calculations are performed for three kinds of signals: (a) the noise-free dynamical variable $x(t)$ of the Lorenz system, (b) the stiff and long duration time evolution of the total current of the electrochemical oscillator Fe–2M H_2SO_4 in the presence of external Ohmic resistance R, and (c) the smooth variation and short duration signal of the same experimental system for a different set of parameters. A comparison between the results of the two algorithms is attempted as well as an investigation of the trends of the Lyapunov spectrum by varying the algorithm, signal, and reconstruction parameters.

PACS number(s): 02.70.−c, 02.60.−x, 05.45.+b

I. INTRODUCTION

An intrinsic property of a large class of relatively low dimensional nonlinear dissipative dynamical systems is the existence of the strange or chaotic attractor in the phase space. The dynamical behavior of such physical systems is studied experimentally by recording an observable function $g(t)$,

$$g(t)=G(\mathbf{x}(t)), \tag{1}$$

where $\mathbf{x}(t)$ is the vector of the dynamical variables of the system, $G:\mathbb{R}^d\rightarrow\mathbb{R}$ is assumed to be a differentiable function and d is the dimension of the system. The observable $g(t)$ is usually sampled at fixed time intervals Δt sec and Δt^{-1} $\sec^{-1}$ denotes the sampling rate of an analog to digital (AD) converter. Therefore, the observable is recorded as a sequence of data points,

$$\{g_1,g_2,\ldots,g_{N_{\max}}\}, \tag{2}$$

sampled at equal time intervals. In (2) $N_{\max}$ denotes the total number of data points whereas $N_{\max}\Delta t=T$ sec is the total sampling time of the observable. The attractor of the dynamical system can be reconstructed from the sequence (2) by using the method of time delay [1].

The chaotic attractor has three main features which distinguish it from any other kind of attractors: (a) nonperiodicity, (b) fractal dimension, and (c) sensitive dependence on the initial conditions (exponential divergence of nearby orbits) [2].

The quantity which characterizes the aperiodicity of the time evolution of a dynamical system is the power spectrum,

$$S(\omega)=\lim_{T\rightarrow\infty}\frac{1}{T}\left|\int_0^T g(s)e^{-i\omega s}ds\right|^2, \tag{3}$$

where ω is the angular frequency and $|\,|$ denotes the modulus of a complex number. The power spectrum $S(\omega)$ can be calculated efficiently by the usual fast Fourier transform (FFT) algorithm [3]. If the time evolution of a dynamical variable is a quasiperiodic function $\mathbf{x}(t)=\mathbf{h}(\omega_1 t,\omega_2 t,\ldots,\omega_k t)$ then the observable $g(t)$ will also be a quasiperiodic function of the same set of frequencies ω_i. In this case, the power spectrum will consist of discrete peaks corresponding to the frequencies $\hat{\omega}_i=\Sigma_{j=1}^{k}\alpha_{ij}\omega_j$. Actually, in experimental situations only the case $k=2$ (or rarely $k=3$) is observed. In contrast, the power spectrum of a chaotic motion will consist of a continuous band due to the aperiodicity of the signal and in principle the quasiperiodic and the chaotic evolution can be distinguished from the power spectrum [4,5]. Nevertheless, the continuous spectrum is easily confused with the power spectrum of an experimental quasiperiodic signal when noise is present. Therefore the aperiodicity can be used only as a gross criterion for the characterization of a chaotic attractor.

The chaotic attractor is characterized not only by the aperiodicity but also from the fact that often is a fractal object. There are several dimensions which give a measure of the fractal character of a chaotic attractor. The most robust quantity calculated directly from the reconstructed attractor is the correlation dimension

$$D_c=\lim_{r\rightarrow 0}\frac{C(r)}{\log r}, \tag{4}$$

where $C(r)$ is a function which counts points of the attractor

having a distance less than r. The correlation dimension D_c is expected to have a noninteger value if the attractor is a fractal set [6].

Although the correlation dimension D_c can be calculated directly from the experimental sequence (2), the procedure suffers from several drawbacks. First, the calculations are very time consuming even though several improvements have been done toward this direction and are already presented in the literature. Second, the procedure calculates a single scalar which often lies very close to an integer value and is influenced by the finite amount and precision of experimental data. This uncertainty of the results make the possible fractal character of the chaotic attractor a poor criterion for the characterization of a large class of experimental signals.

The strongest indication of the existence of chaos is the sensitive dependence on the initial conditions; solutions starting from two points in the phase space separated only infinitesimally are expected to diverge exponentially in time. The sensitive dependence on initial conditions can be considered as the fingerprint of chaos and regarded as an absolute criterion for the distinction of the chaotic motion from any other kind of time evolution. The quantity which expresses the rate of divergence of nearby orbits of a d-dimensional dynamical system and therefore the sensitivity on initial conditions is the Lyapunov exponents λ_i, $i=1,2,\ldots,d$ [4].

The Lyapunov exponents can be used not only for the characterization of a chaotic attractor, obtained numerically or experimentally but also for the calculation of several other quantities. Thus if all positive Lyapunov exponents are known, the metric entropy of the system can be calculated [7],

$$h(\rho)=\int \sum_{\lambda_i>0} \lambda_i(x) m_i(x) \rho(dx), \tag{5}$$

where ρ is a physical measure on the attractor $\lambda_i(x)$ the positive Lyapunov exponents, and $m_i(x)$ their multiplicity. In the case of an ergodic system the Lyapunov exponents are independent of the position in the phase space. If additionally their multiplicity is one, then Eq. (5) takes the form,

$$h(\rho)=\sum_{\lambda_i>0} \lambda_i . \tag{6}$$

The metric entropy $h(\rho)$ gives a measure of the mean rate of creation of information of the system due to the sensitive dependence on initial conditions [4,5].

Another quantity which is directly calculated when the whole spectrum is known, is the Lyapunov or Kaplan-Yorke dimension [8],

$$D_L=k+\frac{\sum_{j=1}^{k}\lambda_j}{|\lambda_{k+1}|}, \tag{7}$$

where $k=\max\{i:\lambda_1+\cdots+\lambda_i>0\}$. The Lyapunov dimension can be considered as a measure of the region of the attractor of high density where most trajectories spend most of the time. The Lyapunov dimension can be considered also as an approximation of the capacity of the attractor even though its value is often smaller than the later.

Finally, in certain cases, the Hausdorff dimension can also be calculated if the Lyapunov spectrum is known [9],

$$D_H=h(\rho)\left(\frac{1}{\lambda_1}+\frac{1}{|\lambda_2|}\right), \quad \lambda_1>0>\lambda_2, \tag{8}$$

where $h(\rho)$ is the metric entropy of the system. Equation (8) holds for a diffeomorphism $f:M^2\rightarrow M^2$, that is, for an invertible and differentiable map of a two dimensional manifold [9].

It can be seen from the above that not only the largest positive exponent but the whole spectrum is important when we are interested in the characterization of a complex signal as well as for the calculation of quantities which express several properties of the attractor.

The three algorithms which are used more often for the calculation of the Lyapunov exponents from the experimental data are the algorithms of Wolf *et al.* [10], Eckmann *et al.* [11], and Sano and Sawada [12]. The algorithm of Wolf *et al.* and similar modifications [13] calculate only the largest exponent, which is positive in the case of a chaotic signal. The calculation of only the positive exponent can cause some difficulties when other criteria for the proper choice of the algorithm parameters are needed. Usually these are the existence of a zero exponent [14] and a negative summation of the exponents. Neither of the above criteria can be used when the Wolf *et al.* algorithm is implemented. Therefore it is difficult to know if the choice of the algorithm parameters, the propagation time, the minimum distance of the neighboring vector and the conservation of the orientation are chosen properly. Additionally, the calculation of any other quantity like the entropy, Lyapunov and information dimension is not possible because the Lyapunov spectrum remains undetermined when the Wolf *et al.* algorithm is implemented.

The Eckmann *et al.* as well as the Sano and Sawada algorithms seem to be the most promising algorithms for the calculation of the Lyapunov spectrum from experimental data. Both algorithms are based on the same key idea: the time evolution of a small sphere defined by the neighboring points of a reference vector of the attractor and the approximate calculation of the tangent matrix propagating small perturbations on the reconstructed attractor's trajectory. The algorithms are easy on the implementation and are based on rather common numerical techniques. Additionally, the parameters of the algorithms are actually only two, the evolution time and the radius of the small sphere. Their proper choice can be tested by seeking always for a zero exponent, a negative divergence of the vector field (negative summation of the Lyapunov exponents), and a plateau region at which the calculated values are independent of the choice of the parameters. Finally, the algorithms converge rather fast, especially when the calculations are performed in a supercomputing environment.

The above mentioned advantages of the Sano and Sawada and the Eckmann *et al.* algorithm is the reason that they are already used by experimentalists in order to characterize

complex signals. The great interest in these algorithms can be also viewed by the large number of improvements of these two algorithms which are presented in the literature [15–22]. Even though the algorithms are already used as tools for the characterization of the dynamical behavior and improvements are also proposed, the original algorithms are not yet investigated thoroughly as a function of their parameters and the features of the experimental signals. Some work was presented concerning the effect of noise on the Lyapunov spectrum when the Sano and Sawada algorithm [23] and the Eckmann *et al.* algorithm [11] are used. It is obvious though, that a detailed investigation of the effect of the various parameters for a variety of signals must be performed before any attempt for improvement of these two algorithms is made. In the present work we implement the two algorithms for a variety of experimental signals with different features and study the trends of the algorithms by varying the parameters of the algorithms. It is shown that the features of the experimental signal is of a great importance for the proper choice of the parameters and in any case they must be chosen thoughtfully and after detailed verification.

In this point we must notice that there is also a different approach for the determination of the Lyapunov exponents from the time series. The procedure is based on the construction of the model equations which reproduce the dynamical behavior and the calculation of the Lyapunov exponents from the resulting equations by using already known algorithms [24]. This procedure will not concern us in the present work.

The purpose of this study is twofold. First, the two algorithms are compared at the formal level in order to reveal their similarities and differences. A special emphasis is paid to express both algorithms in the same mathematical form and elucidated their resemblance through the properties of the mathematical manipulations calculating the Lyapunov spectrum. Second, a detailed study of the role of the algorithm as well as of the signal and reconstruction parameters is attempted in order to explore the trends of the Lyapunov spectrum by varying the parameter values. The effect of the various parameters is examined for three kind of signals with different characteristics. The first system is a noise-free time series obtained numerically by integrating the Lorenz equations,

$$\dot{x} = -\sigma(x-y)$$

,

$$\dot{y} = (\gamma - z)x - y$$

,

$$\dot{z} = xy - bz, \tag{9}$$

for $\sigma=16$, $b=4$, $\gamma=45.92$. The integration of the Lorenz equations was performed by a 4th order Runge-Kutta algorithm with integration step 0.01 and a single precision. The variation of the $x(t)$ variable was used for the determination of the Lyapunov exponents [Fig. 1(a)].

The second signal is obtained experimentally from the electrochemical oscillator Fe–2M H_2SO_4 in the presence of an external ohmic resistance R. The experimental apparatus is described elsewhere [25]. The sampling of the experimental data was carried out by an AD converter for the values of the Ohmic resistance $R=20$ Ω and the applied potential $E=120$ mV. The sampling rate used was 700 sec^{-1} and 120 000 data points were recorded. The mean amplitude of the oscillations is about 15 mA whereas the peak-to-peak time interval varies from 0.05 sec to 0.25 sec [Fig. 1(b)]. This signal can be considered as an extreme case due to its stiffness and small peak-to-peak time interval. We designate this signal as Signal 1 throughout this paper.

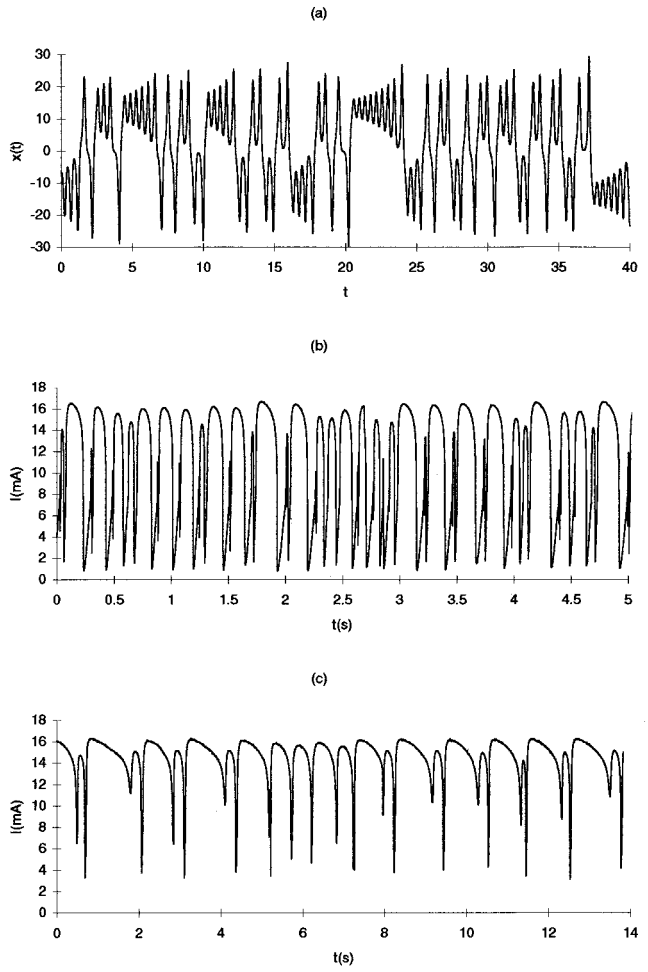

FIG. 1. The three signals used for the calculation of the Lyapunov spectrum. (a) The $x(t)$ variable of the Lorenz system for $\sigma=16$, $b=4$, $\gamma=45.92$; (b) the experimental signal of the system Fe–2M H_2SO_4 for $R=20\,\Omega$, $E=120$ mV (Signal 1), and (c) the experimental signal of the system Fe–2M H_2SO_4 for $R=18$ Ω, $E=0$ mV (Signal 2). Only the first 4000 points are presented.

The third signal is obtained again experimentally from the electrochemical oscillator Fe–2M H_2SO_4 in the presence of the external resistance R. This time the sampling rate used was 290 sec^{-1} and 10 000 data points were recorded. The value of the ohmic resistance was $R=18$ Ω and the applied potential was $E=0$ mV. The mean amplitude of the oscillations is about 15 mA whereas the peak-to-peak time interval varies from 0.5 sec to 1.5 sec [Fig. 1(c)]. We designate this signal as Signal 2 throughout this paper.

The paper is organized as follows: In Sec. II we present some formal aspects of the definition of the Lyapunov exponents. In Sec. III the Sano and Sawada and the Eckmann *et al.* algorithms are presented to some extent and a compari-

son of the two algorithms is attempted. The effect of the algorithm parameters on the Lyapunov spectrum is investigated in Sec. IV. In Sec. V the effect of the time series characteristics is studied. Finally, the effect of the reconstruction parameters of the attractor is presented in Sec. VI. The results are discussed in Sec. VII.

All the calculations were performed in a VAX 9000 main frame computer of the Aristotle University of Thessaloniki, running under VMS 5.5. The codes of both algorithms were written in FORTRAN.

II. DEFINITION OF THE LYAPUNOV EXPONENTS

Before proceeding to a brief description of the Sano and Sawada and the Eckmann *et al.* algorithms it is necessary to define the Lyapunov exponents of a continuous dynamical system which can be described by a set of nonlinear ordinary differential equations,

$$\dot{\mathbf{x}}=\mathbf{f}(\mathbf{x},\boldsymbol{\mu}),\quad \mathbf{x}\in\mathbb{R}^d. \tag{10}$$

In Eq. (10), $\mathbf{x}(t)$ is the vector of the dynamical variables and $\boldsymbol{\mu}$ the vector of parameters. The variational equations of Eq. (10) will be,

$$\dot{\boldsymbol{\xi}}=\mathbf{Df}(\mathbf{x}(t))\boldsymbol{\xi}. \tag{11}$$

where $\boldsymbol{\xi}$ denotes a small perturbation at the orbit point $\mathbf{x}(t)$, $\mathbf{Df}(\mathbf{x}(t))$ is the $d\times d$ matrix with elements $[\partial f_i(\mathbf{x}(t))]/\partial x_j$, $i,j=1,2,\ldots,d$.

The solution of the variational equations in the region of continuity of $\mathbf{Df}(\mathbf{x}(t))$ [26] can be written as,

$$\boldsymbol{\xi}(t)=\mathbf{A}(t,0)\boldsymbol{\xi}(0), \tag{12}$$

where the propagator $\mathbf{A}(t,0)$ satisfies the differential equation,

$$\dot{\mathbf{A}}(t)=\mathbf{Df}(\mathbf{x}(t))\mathbf{A}(t), \tag{13}$$

and the initial condition $\mathbf{A}(0,0)=\mathbf{I}$, where $\mathbf{I}$ is the unit matrix.

For discrete time, i.e., by splitting the interval $[0,t]$ in k discrete time regions, Eq. (12) can be written in the following form,

$$\boldsymbol{\xi}=\mathbf{A}_k\mathbf{A}_{k-1}\cdots\mathbf{A}_2\mathbf{A}_1\boldsymbol{\xi}_0. \tag{14}$$

By inspecting Eq. (14), we observe that the matrix $\mathbf{A}$ can be also written as the matrix product,

$$\mathbf{A}=\mathbf{A}_k\mathbf{A}_{k-1}\ldots\mathbf{A}_2\mathbf{A}_1. \tag{15}$$

The Lyapunov exponents of the system at the orbit point $\mathbf{x}(t)$ are associated with the logarithms of the eigenvalues of the symmetric matrix,

$$\lim_{t\to\infty}\{[\mathbf{A}(t)^T\mathbf{A}(t)]^{1/2}\}=\boldsymbol{\Lambda}. \tag{16}$$

The eigenvalues of $\boldsymbol{\Lambda}$ will have the form $e^{\lambda_j t}$ for $t\to\infty$ and $\mathbf{A}(t)^T$ is the transposed of $\mathbf{A}(t)$ [27]. Let $|\mathbf{e}_j\rangle$ be the right eigenvector corresponding to the eigenvalue $e^{\lambda_j t}$. Then, by definition (dropping the dependence on t for simplicity),

$$\mathbf{A}^T\mathbf{A}|\mathbf{e}_j\rangle=e^{2\lambda_j t}|\mathbf{e}_j\rangle. \tag{17}$$

By multiplying both sides of Eq. (17) with the left eigenvector $\langle\mathbf{e}_j|$, (assuming $\langle\mathbf{e}_i|\mathbf{e}_j\rangle=\delta_{ij}$),

$$\langle\mathbf{e}_j|\mathbf{A}^T\mathbf{A}|\mathbf{e}_j\rangle=e^{2\lambda_j t}. \tag{18}$$

But,

$$\langle\mathbf{e}_j|\mathbf{A}^T\mathbf{A}|\mathbf{e}_j\rangle=\|\mathbf{A}|\mathbf{e}_j\rangle\|^2. \tag{19}$$

By combining Eqs. (18) and (19) we obtain,

$$\|\mathbf{A}|\mathbf{e}_j\rangle\|=e^{\lambda_j t}. \tag{20}$$

Generally, let $E^{(1)}\supset E^{(2)}\supset\cdots\supset E^{(d)}$ be subspaces of $\mathbb{R}^d$ [4]. Then, the Lyapunov exponents are given by,

$$\lambda_j=\lim_{t\to\infty}\frac{1}{t}\ln\|\mathbf{A}(t)\mathbf{e}_j\|,\quad j=1,2,\ldots,d \tag{21}$$

where, $\mathbf{e}_j\in E^{(j)}-E^{(j+1)}$, and $\|\ \|$ denotes any norm [2,4].

If $e^{\mu_j t}$ is an eigenvalue (μ_j complex in general) of the real matrix $\mathbf{A}(t)$ and $|\mathbf{f}_j\rangle$ the corresponding eigenvector, then,

$$\mathbf{A}|\mathbf{f}_j\rangle=e^{\mu_j t}|\mathbf{f}_j\rangle, \tag{22}$$

and by definition,

$$\langle\mathbf{f}_j|\mathbf{A}^T\mathbf{A}|\mathbf{f}_j\rangle=\|\mathbf{A}|\mathbf{f}_j\rangle\|^2. \tag{23}$$

But,

$$\langle\mathbf{f}_j|\mathbf{A}^T\mathbf{A}|\mathbf{f}_j\rangle=e^{\mu_j t}e^{\overline{\mu_j}t}, \tag{24}$$

where $\overline{\mu_j}$ indicates the complex conjugate of μ_j. By combining Eqs. (23) and (24) we obtain

$$\|\mathbf{A}|\mathbf{f}_j\rangle\|=e^{\mathrm{Re}(\mu_j)t}. \tag{25}$$

By comparing Eqs. (20) and (25) we see that the real part of the eigenvalues of the matrix $\mathbf{A}(t)$ are expected to coincide with the eigenvalues of the symmetric matrix $(\mathbf{A}^T\mathbf{A})^{1/2}$, which are always real because this matrix is Hermitian [for a full discussion about the similarities of the eigenvalues and eigenvectors of the matrices $\mathbf{A}(t)$ and $(\mathbf{A}^T\mathbf{A})^{1/2}$ see [28]]. From the above, we notice that if the operator $\mathbf{A}(t)$ is known, the Lyapunov spectrum can be calculated either by the eigenvalues of the matrix $\boldsymbol{\Lambda}$, Eq. (16), or by Eq. (21).

The variational equations Eq. (11) as well as their solution Eq. (12) or Eq. (14) express the stability of the system Eq. (10) under infinitesimal perturbations $\boldsymbol{\xi}$ at the orbit point $\mathbf{x}(t)$. Thus, the Lyapunov exponents can be considered as the rate of convergence or divergence of nearby orbits separated by a small perturbation $\boldsymbol{\xi}$.

III. DESCRIPTION AND COMPARISON OF THE SANO AND SAWADA AND ECKMANN *et al.* ALGORITHMS

From Sec. II we observe that the Lyapunov exponents can be calculated only if the operator $\mathbf{Df}(\mathbf{x}(t))$ or $\mathbf{A}(t)$ is known. If the set of ordinary differential equations describing the dynamical system is known then the calculation can be performed directly since the matrix $\mathbf{Df}(\mathbf{x}(t))$ is directly calcu-

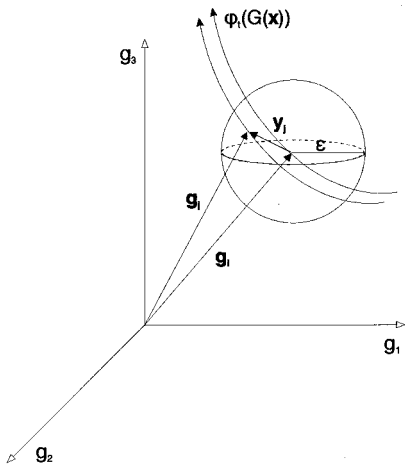

FIG. 2. The construction of the small perturbation vectors $\mathbf{y}_j$ (in the three dimensional space for the sake of visualization). The vector $\mathbf{g}_i$ denotes the reference vector of the orbit $\varphi_t(G(\mathbf{x}))$. The vector $\mathbf{g}_j$ denotes the jth neighbor lying in a sphere of radius ϵ.

lable. On the other hand, when an experiment is performed we actually record only an observable function Eq. (1) or else the sequence (2). It is obvious that in this case the operator $\mathbf{Df}(\mathbf{x}(t))$ is not directly calculable and thus an approximation process must be introduced.

Both the Sano and Sawada and the Eckmann *et al.* algorithms are based on the least-squares approximation of the operator $\mathbf{A}(t)$ in the m-dimensional embedding space. Thus, in order to calculate the Lyapunov spectrum of a d-dimensional system when only the sequence (2) is known, a reconstruction of the attractor must be performed first,

$$\mathbf{g}_\ell = (g_\ell, g_{\ell+\tau}, g_{\ell+2\tau}, \ldots, g_{\ell+(m-1)\tau})^T, \tag{26}$$

where $\ell = 1,2,\ldots,N_{\max}-m+1$ and $m \geqslant 2d+1$ is the embedding dimension, $\tau\Delta t$ sec is the time delay $\tau \in \mathbb{N}^*$.

On the reconstructed attractor Eq. (26), we choose a reference m vector $\mathbf{g}_i$ and form N small m vectors $\mathbf{y}_i$ lying in a m-dimensional hypersphere of radius ε around the reference vector $\mathbf{g}_i$,

$$\mathbf{y}_j = \{(\mathbf{g}_i - \mathbf{g}_j), \|\mathbf{g}_i - \mathbf{g}_j\| \leqslant \epsilon\}, \quad j = 1,2,\ldots,N \tag{27}$$

where $\|\,\|$ indicates the Euclidean norm. If the radius ϵ is chosen to be small, the m vectors $\mathbf{y}_j$ can be considered as small perturbations at the orbit point $\mathbf{g}_i$. Equation (27) indicates that the small m vectors $\mathbf{y}_i$ can be constructed by searching for vectors $\mathbf{g}_j$ laying in a distance $\leqslant\varepsilon$ from the reference point $\mathbf{g}_i$ and forming $\mathbf{y}_j$ as the vector, $\mathbf{g}_i - \mathbf{g}_j$ (Fig. 2).

After a fixed time interval equal to the propagation time $t_p = n\Delta t$ sec, the small m vectors $\mathbf{y}_j$ will be evolved to the m vectors $\mathbf{z}_j$,

$$\mathbf{z}_j = \{(\mathbf{g}_{i+n} - \mathbf{g}_{j+n}), \|\mathbf{g}_i - \mathbf{g}_j\| \leqslant \epsilon\}, \quad j = 1,2,\ldots,N. \tag{28}$$

It can be assumed that the vectors $\mathbf{z}_j$ are generated from the small vectors $\mathbf{y}_j$ by Eq. (14),

$$\mathbf{z}_j = \mathbf{A}_i \mathbf{y}_j, \tag{29}$$

where the $m \times m$ matrix $\mathbf{A}_i$ is the approximation of the operator $\mathbf{A}(t,0)$ at the orbit point $\mathbf{g}_i$. The matrix $\mathbf{A}_i$ can be determined numerically by solving the minimization problem,

$$\min_{A_i} S = \min_{A_i} \frac{1}{N} \sum_{j=1}^{N} \|\mathbf{z}_j - \mathbf{A}_i \mathbf{y}_j\|^2. \tag{30}$$

The minimization problem Eq. (30) can be solved by utilizing a linear-least-squares procedure either by solving the normal equations (e.g., by Gauss elimination) or by applying Householder transformations [3].

Up to this point both algorithms follow the above procedure in order to determine the operator $\mathbf{A}_i$. The Sano and Sawada algorithm proceeds as follows:

(a) Operation of $\mathbf{A}_i$ on an orthonormal set of vectors $\{\mathbf{e}_j^{(i)}\}$, $j = 1,2,\ldots,m$.

(b) Production of a new set $\{\mathbf{e}_j^{(i+n)}\}$ by orthonormalizing the vectors $\{\mathbf{A}_i \mathbf{e}_j^{(i)}\}$.

(c) Calculation of the Lyapunov spectrum from an equation analogous to Eq. (21),

$$\lambda_j = \frac{1}{k t_p} \sum_{i=1}^{k} \log \|\mathbf{A}_i \mathbf{e}_j^{(i)}\| \tag{31}$$

and propagation to the next point $\mathbf{g}_{i+n}$ (vector after propagation time $t_p = n\Delta t$).

The procedure is expected to converge to the Lyapunov spectrum for $k \to \infty$ because the orthonormal set $\{\mathbf{e}_j^{(i)}\}$ defines subspaces $E_{(1)} = \text{span}\{\mathbf{e}_j^{(i)}, \mathbf{e}_{j+1}^{(i)}, \ldots, \mathbf{e}_{j+n}^{(i)}\}$, $E^{(2)} = \text{span}\{\mathbf{e}_{j+1}^{(i)}, \mathbf{e}_{j+2}^{(i)}, \ldots, \mathbf{e}_{j+n}^{(i)}\}, \ldots,$ $E^{(m)} = \text{span}\{\mathbf{e}_{j+n}^{(i)}\}$.

The Eckmann *et al.* algorithm also approximates the operator $\mathbf{A}_i$ by Eq. (30). In order to calculate the eigenvalues of the matrix $\mathbf{\Lambda}$ [Eq. (16)] proceeds by the following steps:

(a) Factorization of the matrix $\mathbf{A}_i \mathbf{Q}_{i-1}$ by utilizing the QR decomposition technique [3,29],

$$\mathbf{A}_i \mathbf{Q}_{i-1} = \mathbf{Q}_i \mathbf{R}_i, \quad i = 1,2,\ldots,k \tag{32}$$

where $\mathbf{Q}_i$ is an orthogonal matrix, $\mathbf{R}_i$ is an upper triangular matrix, and $\mathbf{Q}_o = \mathbf{I}$. The decomposition, Eq. (32) is unique as far as the matrix $\mathbf{A}_i \mathbf{Q}_{i-1}$ is invertible. The decomposition can be utilized, in principle, either by using the Gramm-Schmidt orthonormalization procedure or the Householder transformations [3,29]. The operator $\mathbf{A} = \mathbf{A}_k \mathbf{A}_{k-1} \cdots \mathbf{A}_2 \mathbf{A}_1$ is expected to converge to the upper triangular matrix,

$$\mathbf{A} = \mathbf{R}_k \mathbf{R}_{k-1} \mathbf{R}_{k-2} \cdots \mathbf{R}_2 \mathbf{R}_1, \quad k \to \infty. \tag{33}$$

(b) Calculation of the Lyapunov spectrum from the diagonal elements of $\mathbf{R}_i$, (eigenvalues of $\mathbf{A}$), i.e.,

$$\lambda_j = \frac{1}{k t_p} \sum_{i=1}^{k} \log R_i^{(j,j)} \tag{34}$$

and propagation to the next vector $\mathbf{g}_{i+n}$, (vector after propagation time $t_p = n\Delta t$).

From the description of the procedure followed by both algorithms we observe that the calculated values of the

Lyapunov exponents strongly depend on six parameters. The construction of the small m vectors $\mathbf{y}_i$ depends on the choice of the radius ϵ which expresses the neighborhood of the reference orbit point $\mathbf{g}_i$. The calculation of the values of the Lyapunov exponents depends also on the choice of the propagation time $t_p = n\Delta t$, which expresses the time interval in which the divergence or convergence of nearby orbits is studied. We call the radius ϵ and the propagation time t_p the algorithm parameters.

Additionally, the calculated Lyapunov spectrum depends on two parameters concerning the recorded signal. These parameters are the total number of data points $N_{\max}$ and the sampling rate Δt^{-1}. These two parameters are denoted as the signal parameters.

Finally, the Lyapunov exponents are calculated in a suitable reconstructed space and thus the calculated values depend on the choice of the embedding dimension m and the time delay τ which are denoted as the reconstruction parameters.

In order to investigate the similarities and differences of the two algorithms, let us describe the Sano and Sawada algorithm by using a notation similar to the notation used by Eckmann *et al.*

Let $\mathbf{e}_1^{(0)}=(1,0,...,0)^T$, $\mathbf{e}_2^{(0)}=(0,1,...,0)^T$,..., $\mathbf{e}_m^{(0)}=(0,0,\ldots,1)^T$ be an initially chosen orthonormal set of vectors. Denote by $\mathbf{Q}_o$ the matrix having as columns the vectors $\mathbf{e}_i^{(0)}$,

$$\mathbf{Q}_o=[\mathbf{e}_1^{(0)},\mathbf{e}_2^{(0)},\ldots,\mathbf{e}_m^{(0)}]=\mathbf{I}, \tag{35}$$

where $\mathbf{I}$ is the unit matrix. Let us denote by $\mathbf{U}_1$, the operation of the operator $\mathbf{A}_1$ to every element of the set $\{\mathbf{e}_j^{(0)}\}$,

$$\mathbf{A}_1\mathbf{Q}_o=\mathbf{U}_1\equiv[\mathbf{u}_1^{(1)},\mathbf{u}_2^{(1)},\ldots,\mathbf{u}_m^{(1)}]. \tag{36}$$

Now, consider a new orthonormal set of vectors $\{\mathbf{e}_j^{(1)}\}$ which are column vectors of a new orthogonal matrix $\mathbf{Q}_1$, produced by the orthonormalization of the vectors $\mathbf{u}_i^{(1)}\equiv\mathrm{col}_i(\mathbf{U}_1)$,

$$\mathbf{Q}_1=[\mathbf{e}_1^{(1)},\mathbf{e}_2^{(1)},\ldots,\mathbf{e}_m^{(1)}], \tag{37}$$

and form the product $\mathbf{A}_2\mathbf{Q}_1$. By applying the above procedure k times we obtain,

$$\mathbf{A}_k\mathbf{Q}_{k-1}=\mathbf{U}_k\equiv[\mathbf{u}_1^{(k)},\mathbf{u}_2^{(k)},\ldots,\mathbf{u}_m^{(k)}]. \tag{38}$$

For $\kappa\to\infty$ the Lyapunov spectrum will be given by,

$$\lambda_j=\frac{1}{kt_p}\sum_{i=1}^{k}\log\|\mathbf{u}_j^{(i)}\| \tag{39}$$

because $\mathbf{u}_j^{(i)}\in E^{(j)}-E^{(j+1)}$ (subspaces are defined as in Sec. III B). It is obvious that Eq. (39) is equivalent to Eq. (31).

In a similar notation, the Eckmann *et al.* algorithm starts the calculations by choosing a matrix (the unit matrix),

$$\mathbf{Q}_o=\mathbf{I}, \tag{40}$$

and calculating the decomposition,

$$\mathbf{A}_1\mathbf{Q}_o=\mathbf{Q}_1\mathbf{R}_1\equiv\mathbf{U}_1, \tag{41}$$

where $\mathbf{R}_1$ is an upper triangular matrix and $\mathbf{Q}_1$ is an orthogonal matrix obtained by the orthonormalization of $\mathrm{col}_i(\mathbf{A}_1\mathbf{Q}_o)\equiv\mathbf{u}_i^{(1)}$ (or similarly by the Householder transformation of the matrix $\mathbf{A}_1\mathbf{Q}_0$). By applying the above procedure κ times we obtain,

$$\mathbf{A}_k\mathbf{Q}_{k-1}=\mathbf{Q}_k\mathbf{R}_k\equiv\mathbf{U}_k, \tag{42}$$

where $\mathbf{R}_k$ is an upper triangular matrix and $\mathbf{Q}_k$ is an orthogonal matrix obtained by the orthonormalization of $\mathrm{col}_i(\mathbf{A}_k\mathbf{Q}_{k-1})$. But the matrix $\mathbf{A}$ will be given by the product of Eq. (15). By replacing the matrices $\mathbf{A}_i$, $i=1,2,\ldots,k$, in Eq. (15) we obtain,

$$\mathbf{A}=\mathbf{Q}_k\mathbf{R}_k\mathbf{R}_{k-1}\cdots\mathbf{R}_2\mathbf{R}_1, \tag{43}$$

where for $k\to\infty$,$\mathbf{Q}_k\to\mathbf{I}$ [29]. The product of upper triangular matrices is an upper triangular matrix and the determinant of an upper triangular matrix equals to the product of its diagonal elements. Therefore, the eigenvalues of $\mathbf{A}$ will be the diagonal elements of the product (43) for $k\to\infty$. Thus, the Lyapunov exponents are given by,

$$\lambda_j=\frac{1}{kt_p}\log\prod_{i=1}^{k}R_i^{(j,j)}, \tag{44}$$

or by Eq. (34) for computational reasons, under the restriction that the real part of the eigenvalues of $\mathbf{A}$ coincide with the eigenvalues of $(\mathbf{A}^T\mathbf{A})^{1/2}$ [28].

By inspecting Eqs. (38) and (42), for $k=i$ we notice that,

$$\mathbf{U}_i=\mathbf{Q}_i\mathbf{R}_i, \tag{45}$$

that is, the matrix $\mathbf{U}_i$ is transformed to the upper triangular matrix $\mathbf{R}_i$ via an orthogonal transformation. But orthogonal transformations preserve norms and thus we expect,

$$\|\mathbf{u}_j^{(i)}\|=\|\mathrm{col}_j(\mathbf{R}_i)\|,\quad j=1,2,\ldots,m. \tag{46}$$

Let us compare the column vectors of $\mathbf{U}_i$ and $\mathbf{R}_i$ one by one,

$$\|\mathbf{u}_1^{(i)}\|=\|\mathrm{col}_1(\mathbf{R}_i)\|\equiv R_i^{(1,1)}, \tag{47}$$

and,

$$\|\mathbf{u}_j^{(i)}\|=\|\mathrm{col}_j(\mathbf{R}_i)\|\neq R_i^{(j,j)},\quad j>2. \tag{48}$$

Equation (47) indicates that we should expect both algorithms to give identical results of the largest Lyapunov exponent λ_1, because the Sano and Sawada algorithm calculates λ_1 by summing the logarithms of $\|\mathbf{u}_1^{(j)}\|$, $j=1,2,\ldots,k$ and the Eckmann *et al.* algorithm by summing the logarithms of the matrix elements $R_i^{(1,1)}$. As far as it concerns the rest of the spectrum, we expect a mismatch. The Sano and Sawada algorithm calculates λ_j as the summation of the logarithms of $\|\mathbf{u}_i^{(j)}\|$, $j>2$ and the Eckmann *et al.* algorithm by the summation of the logarithms of the matrix elements $R_i^{(jj)}$. Equation (48) indicates that these two quantities will be unequal.

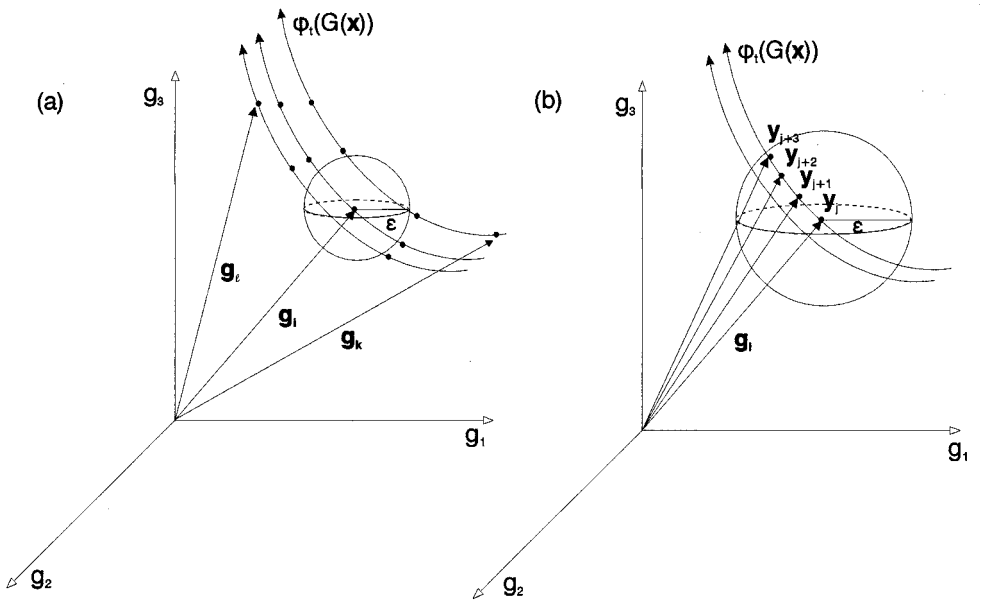

FIG. 3. (a) The effect of the choice of the small radius ε. No points are laying in the sphere of radius ε. (b) The effect of large radius ε. All points are laying on the same orbit and thus the vectors $\mathbf{y}_j$ do not represent the small perturbation on the orbit point $\mathbf{g}_i$.

IV. STUDY OF THE ALGORITHM PARAMETERS ε, t_p

A. The effect of the radius ε

In order to form the small vectors $\mathbf{y}_j$ of the tangent space at a given reference point of the embedding space defined by the vector $\mathbf{g}_i$ and study their evolution after a finite propagation time both Sano and Sawada and Eckmann *et al.* algorithms search for N neighboring vectors $\mathbf{g}_j$, $j=1,2,\ldots,N$, within a m-dimensional hypersphere of radius ε.

In general, the radius ε of the m sphere must be small enough in order for the vectors $\mathbf{y}_j=\mathbf{g}_i-\mathbf{g}_j$ to be small and the tangent space approximation to be fulfilled. Of course, while we are dealing with experimentally obtained time series instrumental and system noise as well as noise due to round-off errors is always present. For this reason ε must be greater than the noise level of the system. The use of an extremely small ε may also cause an incapability to determine $N \geqslant m$ neighboring vectors; if the sphere defined by ε is very small it may be impossible to find N vectors satisfying the condition, $\|\mathbf{g}_i-\mathbf{g}_j\| \leqslant \varepsilon$ [Fig. 3(a)]. At this point, it must be noticed that the number N of small vectors $\mathbf{y}_j$ must be greater than m in order to avoid poor estimation of the least-squares procedure.

However the use of large ε will lead to the construction of neighboring vectors which will not belong to the tangent space at the orbit point $\mathbf{g}_i$ and thus, the hypothesis that the vectors $\mathbf{y}_j$ represent infinitesimal perturbations at this orbit point will not hold. Additionally, the use of large ε will cause the algorithms to locate all the neighboring vectors on the same trajectory. Therefore, the vectors $\mathbf{y}_j$ will not represent initial perturbations at the reference point $\mathbf{g}_i$ [Fig. 3(b)].

The terms ''small'' and ''large'' are used, though, somehow ambiguously. Often, it is useful to express the magnitude of the radius ε as the fraction $\varepsilon/\varepsilon_A$, where ε_A is the mean or approximate radius of the reconstructed attractor. Nevertheless, the permitted values of ε will depend also on the embedding dimension m chosen for the reconstruction of the attractor. If it is assumed that the attractor is reconstructed in the m-dimensional space, the norm of any vector will be,

$$\|\mathbf{g}_i\| = \left(\sum_{j=0}^{m-1} g_{i+j\tau}^2 \right)^{1/2}. \tag{49}$$

It can be seen from Eq. (49) that the norm of any vector depends on the embedding dimension m. Higher embedding dimensions cause more extensive attractors. Therefore as the embedding dimension increases the permitted values of ε are increasing, too.

The effect of ε can be studied by varying ε while keeping all the other parameters constant (the values of the constant parameters are shown in Table I). The effect of ε on the values of the Lyapunov spectrum of the Lorenz signal using the Sano and Sawada algorithm is shown in Fig. 4(a). In this figure we observe that the Sano and Sawada algorithm gives stable results (i.e., independent of the variation of the parameters) for the positive λ_1 and zero exponent λ_2, for a large region of ε values, $1 \leqslant \varepsilon < 8$ or $0.02 \leqslant \varepsilon/\varepsilon_A < 0.16$, (where $\varepsilon_A \approx 50$). In contrast, the negative exponent λ_3 seems to be very subjective to the choice of the radius ε. Thus, only for

TABLE I. Parameters used for the calculation of the Lyapunov spectra of the Lorenz signal, Signal 1 and Signal 2. When one of the parameters was varied all the others were kept constant. (*) denotes when the Sano and Sawada algorithm is used. (**) denotes when the Eckmann *et al.* algorithm is used.

	Lorenz signal	Signal 1	Signal 2
ε	1	8	7
t_p	0.1	1.428 s	0.034 s
$N_{\max}$	120 000	120 000	100 00
Δt	0.01	1/700 s	1/290 s
m	$3^{(*)}$, $5^{(**)}$	7	7
τ	10	3	3

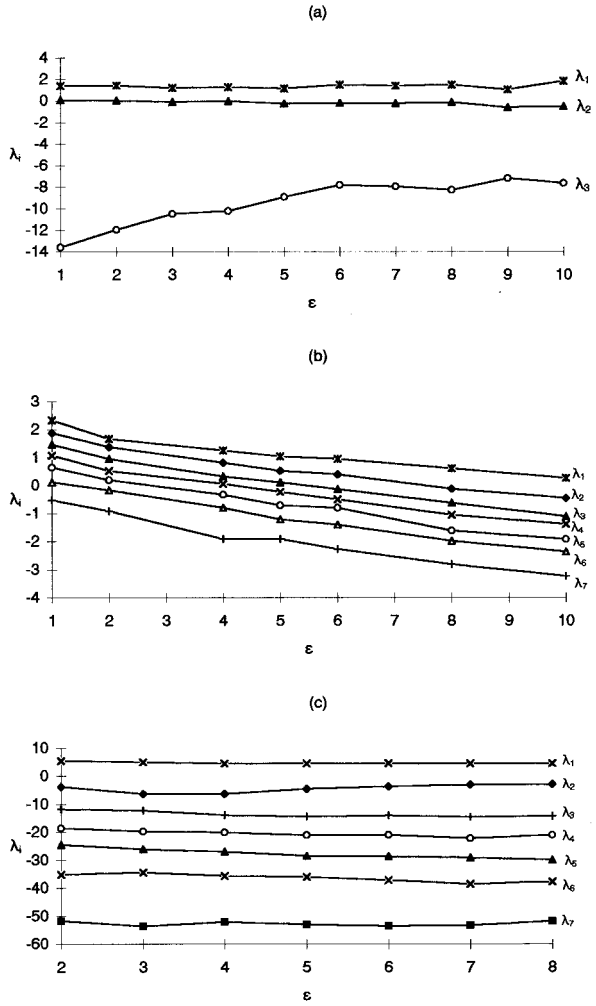

FIG. 4. The effect of the radius ε on the results of the Sano and Sawada algorithm. (a) Effect of ε on the Lyapunov spectrum of the Lorenz signal; (b) effect of ε on Signal 1, and (c) effect of ε on Signal 2.

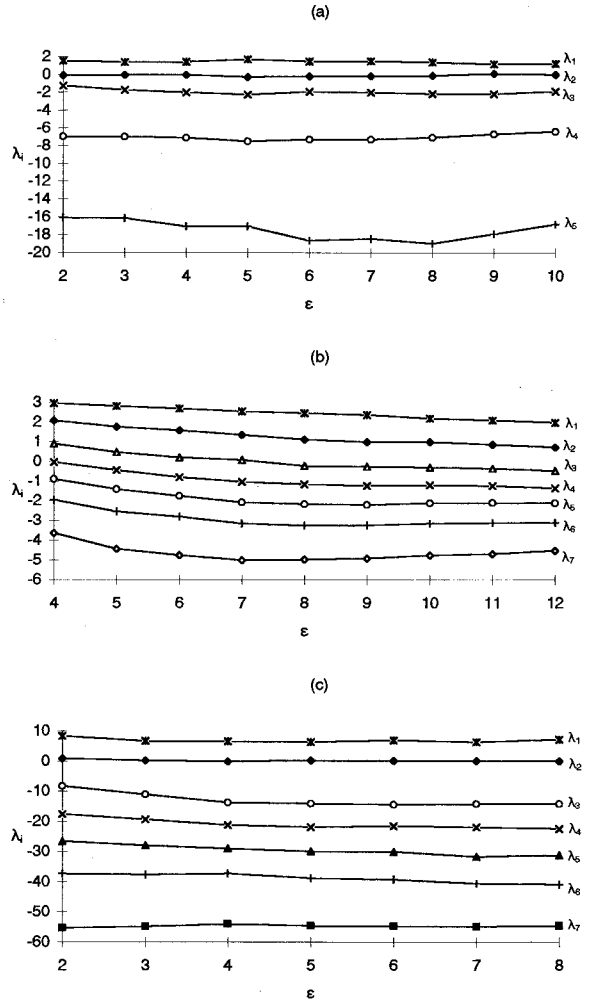

FIG. 5. The effect of the radius ε on the results of the Eckmann *et al.* algorithm. (a) Effect of ε on the Lyapunov spectrum of the Lorenz signal; (b) effect of ε on Signal 1, and (c) effect of ε on the Signal 2.

very small values $\varepsilon<2$ it approaches (but it never reaches) the theoretically calculated value.

A different effect is observed for the stiff Signal 1. For small values $\varepsilon<4$ the calculated values of the exponents are extremely large and can be rejected because the summation of the exponents, i.e., the divergence of the vector field $\Sigma_{j=1}^{m}\lambda_j \approx \partial \mathbf{f}(\mathbf{x})$ is a positive number which is unacceptable for the dissipative system Fe–2M H_2SO_4. The extremely large values of the exponents for small ε can be attributed to the significant presence of noise for small values of the radius, ε. For $3<\varepsilon<7$ or $0.13<\varepsilon/\varepsilon_A<0.30$ (where $\varepsilon_A \approx 23$) a plateau is observed. For $\varepsilon>7$ the calculated values are subjected to small changes of ε possibly due to the fact that the m vectors $\mathbf{y}_i$ can not be considered as small anymore [Fig. 4(b)].

In Fig. 4(c) the ε dependence of the Lyapunov spectrum for the smooth Signal 2 is presented. As can be seen, the spectrum is very stable to changes of the parameter ε even though the zero exponent is not well approximated. The values of λ_i are forming a plateau for $4\leqslant\varepsilon\leqslant8$ or $0.18\leqslant\varepsilon/\varepsilon_A\leqslant0.36$ (where $\varepsilon_A \approx 22$).

In contrast with the Sano and Sawada algorithm, the Eckmann *et al.* algorithm seems to be more stable to small changes of the radius ε even for the negative Lyapunov exponent of the Lorenz system, as it can be seen from Fig. 5(a). In this figure we notice that the spectrum is more or less stable for $2\leqslant\varepsilon\leqslant8$ or $0.03\leqslant\varepsilon/\varepsilon_A\leqslant0.12$ (where $\varepsilon_A \approx 65$). For largest values of ε the spectrum increases possibly due to the large magnitude of the vectors $\mathbf{y}_i$. Additionally, the calculated value of the negative Lyapunov exponents lie very close to the theoretical ones.

A similar trend with that of the Sano and Sawada algorithm is observed for the stiff experimental Signal 1. For small values $\varepsilon<7$ the exponents are very large and subjected to small changes of ε. For $7\leqslant\varepsilon\leqslant10$ $(0.30\leqslant\varepsilon/\varepsilon_A\leqslant0.44)$ a plateau is observed where the spectrum is more or less stable. For $\varepsilon>10$ an increase of the exponents is observed due to the large norm of the vectors $\mathbf{y}_i$ [Fig. 5(b)].

Finally, the Lyapunov spectrum of Signal 2 is very stable for increasing values of ε, especially for $4\leqslant\varepsilon\leqslant7$ $(0.18\leqslant\varepsilon/\varepsilon_A\leqslant0.32)$ where a plateau is observed. The zero exponent is also calculated with good accuracy as it can be seen in Fig. 5(c).

We must have in mind that as far as it concerns the experimental signals the noise due to the AD converter is 0.005

mA, about 0.033% of the experimental signal's amplitude. Additionally, the noise due the potensiostat is 0.03 mA, 0.2% of the amplitude of the experimental signal. As a consequence, by using a radius ε close to this noise level we expect a deviation for the true values.

B. The effect of the propagation time t_p

The propagation time $t_p = n\Delta t$, where $n \in \mathbf{N}^*$, may be the most crucial parameter of both algorithms; the results of both algorithms are highly subjected to the choice of the propagation time. As it can be seen from Eqs. (31) and (34) for very small propagation time the calculated Lyapunov exponents will be extremely large due to the value of the term, t_p^{-1}. One might think that for $k \to \infty$ the term kt_p in Eqs. (31) and (34) would become small and thus the true values of λ_j could be calculated. The true calculation of λ_j cannot be performed even for large values of k, because k serves only for the calculation of the mean exponential divergence or convergence of the nearby orbits.

The effect of the propagation time on the Lyapunov spectrum can be studied by varying t_p for fixed values of the rest of the parameters, shown in Table I. The dependence of the Lyapunov spectrum of the Lorenz system on t_p when the Sano and Sawada algorithm is implemented, is presented in Fig. 6(a). It can be seen that for small values of the propagation time, $t_p < 0.04$, the calculated values of the exponents are very large. A plateau is observed for $0.04 \leqslant t_p \leqslant 0.08$ where the exponents are more or less stable to changes of the propagation time.

In Fig. 6(b) the dependence of the Lyapunov spectrum on the propagation time for Signal 1 is presented. For $t_p < 1.43$ sec the spectrum is highly subjected to changes of the propagation time. In contrast, for 1.43 sec $\leqslant t_p \leqslant 1.86$ sec a plateau is formed and the Lyapunov exponents attain a stable value.

A similar effect is observed for the smooth Signal 2, as it is shown in Fig. 6(c). For $t_p < 0.035$ sec the spectrum does not attain stable values for increasing propagation time. For 0.035 sec $< t_p < 0.049$ sec a plateau is formed and the Lyapunov exponents attain a stable value, even though a zero exponent is not well determined.

The dependence of the Lyapunov spectrum of the Lorenz signal on the propagation time using the Eckmann *et al.* algorithm is similar with the one for the Sano and Sawada algorithm. This can be seen in Fig. 7(a) where for small values of the propagation time $t_p \leqslant 0.03$ the calculated exponents depend on the chosen value of the propagation time. For $0.03 \leqslant t_p \leqslant 0.06$ a plateau is formed where the exponents are independent of the propagation time. For increasing t_p an increase of the spectrum also takes place.

A great similarity of the effect of t_p on the Lyapunov exponents is observed for both algorithms also in the case of the stiff experimental Signal 1. As it can be seen in Fig. 7(b) for $t_p \leqslant 0.657$ sec the spectrum is irregularly subjected to the changes of the propagation time. For 0.657 sec $< t_p \leqslant 0.920$ sec a plateau is formed where the Lyapunov exponents attain a value which does not depend on the choice of t_p.

The dependence of Signal 2 is shown in Fig. 7(c). For $t_p < 0.021$ sec the Lyapunov exponents depend on changes of propagation time. For 0.021 sec $\leqslant t_p \leqslant 0.042$ sec a plateau is formed where the Lyapunov exponents attain fixed values which do not depend strongly on the choice of the propagation time.

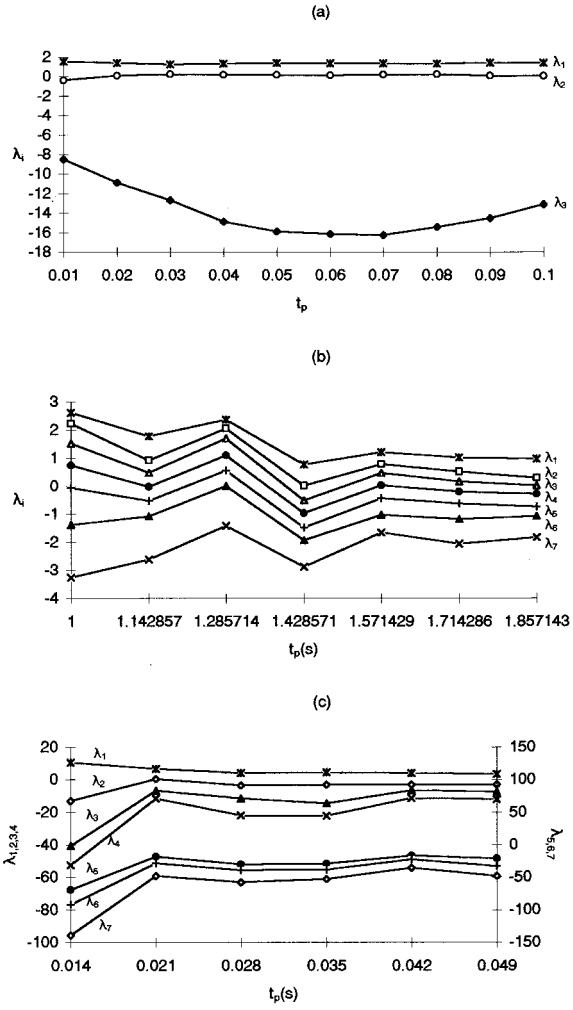

FIG. 6. The effect of the propagation time t_p on the results of the Sano and Sawada algorithm. (a) Effect of t_p on the Lyapunov spectrum of the Lorenz signal; (b) effect of t_p on Signal 1, and (c) effect of t_p on Signal 2.

V. STUDY OF THE SIGNAL PARAMETERS $N_{\max}$, Δt

A. The effect of the number of data points $N_{\max}$

The number of total data points is very important for the reliable determination of the Lyapunov spectrum. J.-P. Eckmann and D. Ruelle [30] demand $N_{\max} = 10^{m/2}$ points for the evaluation of the dimension of the attractor and $N_{\max} = 10^m$ for the calculation of the Lyapunov exponents. This means that if the embedding dimension used is 4 then the required number of points will be 10^4. Sano and Sawada [12] require $N_{\max} = 3 \times 10^4 - 14 \times 10^4$ points for the same embedding dimension.

In practice, the total number of points must be large in order to obtain a dense attractor in the embedding space. As the embedding dimension increases the attractor becomes larger Eq. (49) and thus the required number of data points $N_{\max}$ increases, too, in order to maintain a dense enough attractor. It is obvious that the total number of experimental

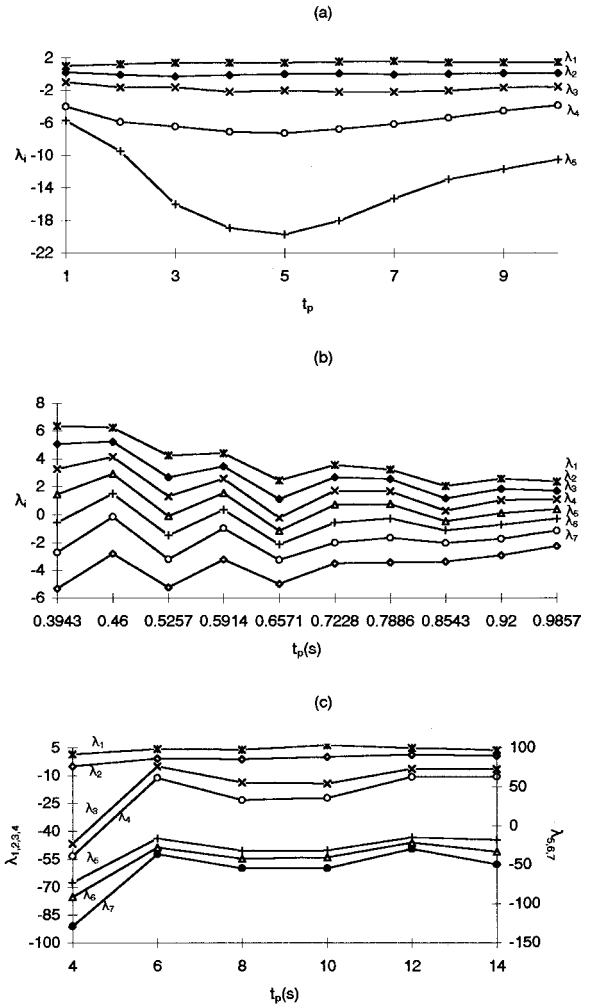

FIG. 7. The effect of the propagation time t_p on the results of the Eckmann *et al.* algorithm. (a) Effect of t_p on the Lyapunov spectrum of the Lorenz signal; (b) effect of t_p on Signal 1, and (c) effect of t_p on Signal 2.

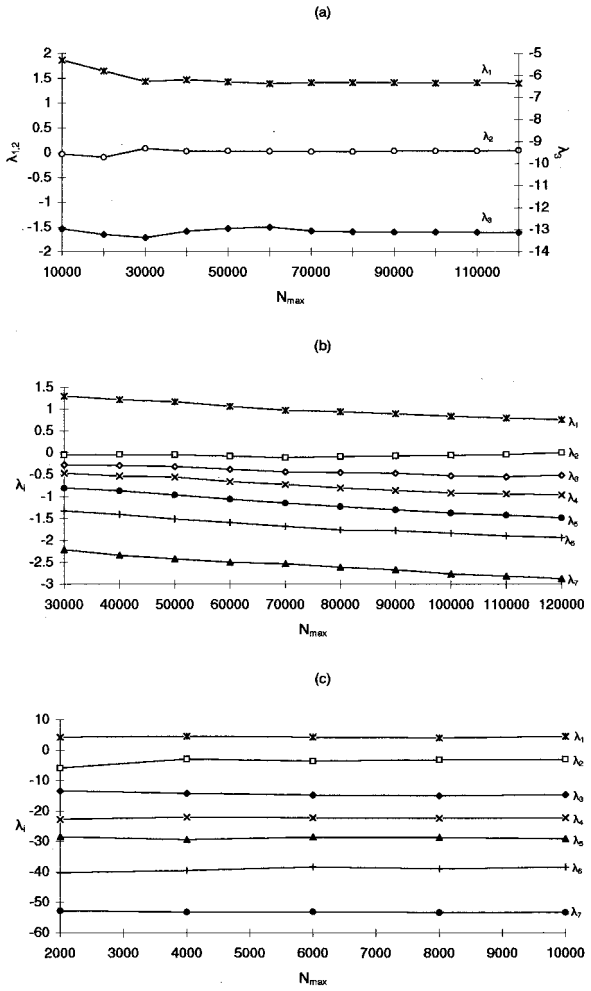

FIG. 8. The effect of the maximum number of data points $N_{\max}$ on the results of the Sano and Sawada algorithm. (a) Effect of $N_{\max}$ on the Lyapunov spectrum of the Lorenz signal; (b) effect of $N_{\max}$ on Signal 1, and (c) effect of $N_{\max}$ on Signal 2.

points $N_{\max}$ must be large by means of a large total sampling time and not due to the increase of the sampling rate.

In order to study the effect of $N_{\max}$ all other parameters are kept constant (Table I) and $N_{\max}$ is varied. The effect of $N_{\max}$ on the Lyapunov exponents of the Lorenz system, when the Sano and Sawada algorithm is used, is presented in Fig. 8(a). As it can be seen, the calculated spectrum is stable for values $N_{\max} \geqslant 30\,000$ data points. The deviation of the Lyapunov spectrum from the true values becomes large for smaller values of $N_{\max}$ where the reconstructed attractor is not dense enough.

As it is presented in Fig. 8(b) the Lyapunov spectrum of Signal 1 is more sensitive to changes of $N_{\max}$. Thus we observe an increase of all nonzero exponents for the decreasing values of $N_{\max}$. The increase of the values of the exponents becomes large for $N_{\max} < 80\,000$ points.

The Lyapunov spectrum of the smooth experimental Signal 2 is very stable even for very small values of the parameter $N_{\max}$. This is shown Fig. 8(c) where for $N_{\max} > 4000$ points, the spectrum attains a fixed value which is not subjected to changes of the total number of experimental points.

The Eckmann *et al.* algorithm seems to be very stable and precise even for very small values of the parameter $N_{\max}$ as far as it concerns the noise-free time series obtained from the Lorenz equations. Thus even for $N_{\max} = 10\,000$ points the calculated values of the Lyapunov exponents for the Lorenz system remain very close to the theoretical values Fig. 9(a).

In contrast with the great stability of the Eckmann *et al.* algorithm for the Lorenz signal, the situation is somehow different for Signal 1 and seems similar to the results of the Sano and Sawada algorithm. Thus, for $N_{\max} < 80\,000$ points the Lyapunov exponents tend to become very sensitive to the decrease of the number of data points Fig. 9(b).

By decreasing the number of points of Signal 2 we observe that the calculated values of the Lyapunov exponents do not change for $N_{\max} \geqslant 4000$ points. The dependence of the Lyapunov spectrum on $N_{\max}$, using the Eckmann *et al.* algorithm can be seen in Fig. 9(c).

B. The effect of the sampling rate, Δt^{-1}

As it was mentioned in Sec. V A the total number of points must be large in the sense of a large total sampling time and not of an extremely large value of the sampling

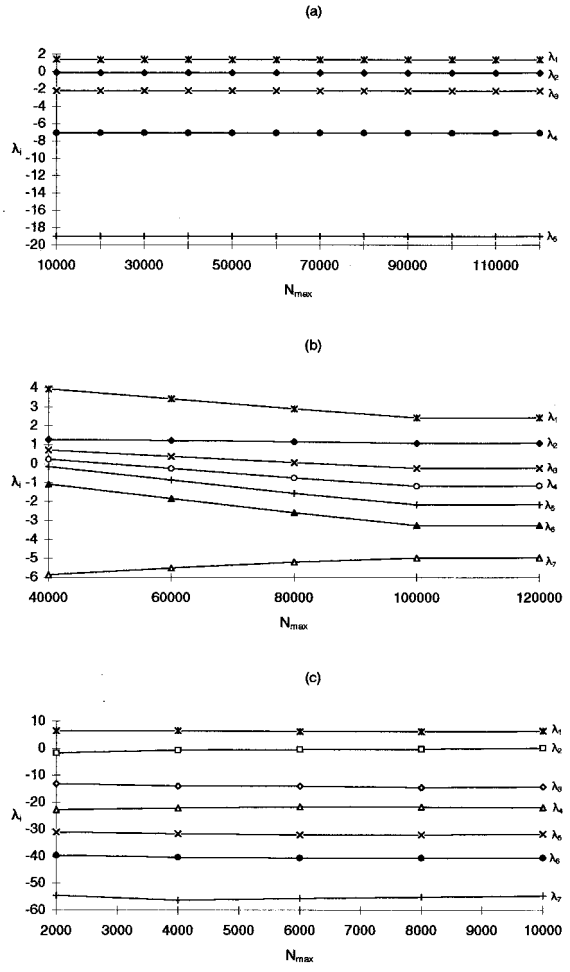

FIG. 9. The effect of the maximum number of data points $N_{\max}$ on the results of the Eckmann *et al.* algorithm. (a) Effect of $N_{\max}$ on the Lyapunov spectrum of the Lorenz signal; (b) effect of $N_{\max}$ on Signal 1, and (c) effect of $N_{\max}$ on Signal 2.

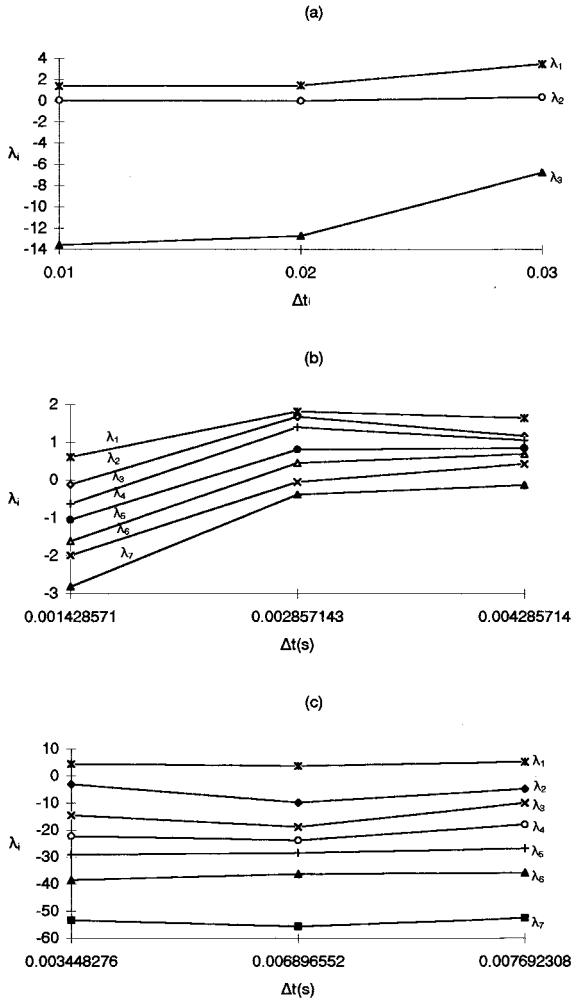

FIG. 10. The effect of the sampling rate Δt^{-1} on the results of the Sano and Sawada algorithm. (a) Effect of Δt^{-1} on the Lyapunov spectrum of the Lorenz signal; (b) effect of Δt^{-1} on Signal 1, and (c) effect of Δt^{-1} on Signal 2.

rate. The choice of a very large sampling rate Δt^{-1} causes three problems. First, it leads to the false feeling that the total number of experimental points are enough for the true determination of the Lyapunov spectrum. Second, the determined small vectors $\mathbf{y}_j$ will mainly lie on the same orbit [Fig. 3(b)] and so they will not represent vectors in the tangent space. Finally, an extreme value of Δt^{-1} will cause an overestimation of the spectrum due to the large value of the term $n\Delta t$.

These three reasons indicate that the choice of the proper sampling rate is actually crucial and has to be studied carefully. Of course it must be considered that the sampling rate must be large enough in order to capture all the features of the experimental signal. In the present section we attempt a brief study of the effect of Δt^{-1} for the three signals under study, for three different values of the sampling rate. We did not perform different experiments to obtain signals for a different sampling rate of the AD converter but we used the same experimental signals by sampling points in a different rate. This was done in order to ensure that we are dealing with exactly the same experimental signals.

The effect of the sampling rate was studied by keeping all other parameters constant (Table I) and varying Δt^{-1}. The effect of the sampling rate on the Lyapunov spectrum of the Lorenz system, using the Sano and Sawada algorithm, is presented in Fig. 10(a) for three different values of Δt^{-1}. As can be seen, the Lyapunov spectrum tends to have higher values for the increasing values of Δt (decreasing Δt^{-1}). A similar shift is observed for the stiff experimental Signal 1 Fig. 10(b). For large values of Δt we do not expect to calculate the true values of the Lyapunov exponents because many features of the experimental signal are not captured due to the stiffness of the signal. In contrast, the Lyapunov spectrum is well determined for Signal 2 due to the smoothness of the time series Fig. 10(c).

Similar trends are observed also when the Eckmann *et al.* algorithm is implemented. Large sampling rates cause false values of the Lyapunov exponents of the Lorenz signal as well as for Signal 1. The effect of the choice of Δt for these two signals can be seen in Figs. 11(a) and 11(b). In contrast, the Lyapunov spectrum remains fairly constant for three different values of Δt in the case of the smooth Signal 2 [Fig. 11(c)]. In this figure we observe that only a small increase takes place as Δt increases while the positive and zero exponents remain constant.

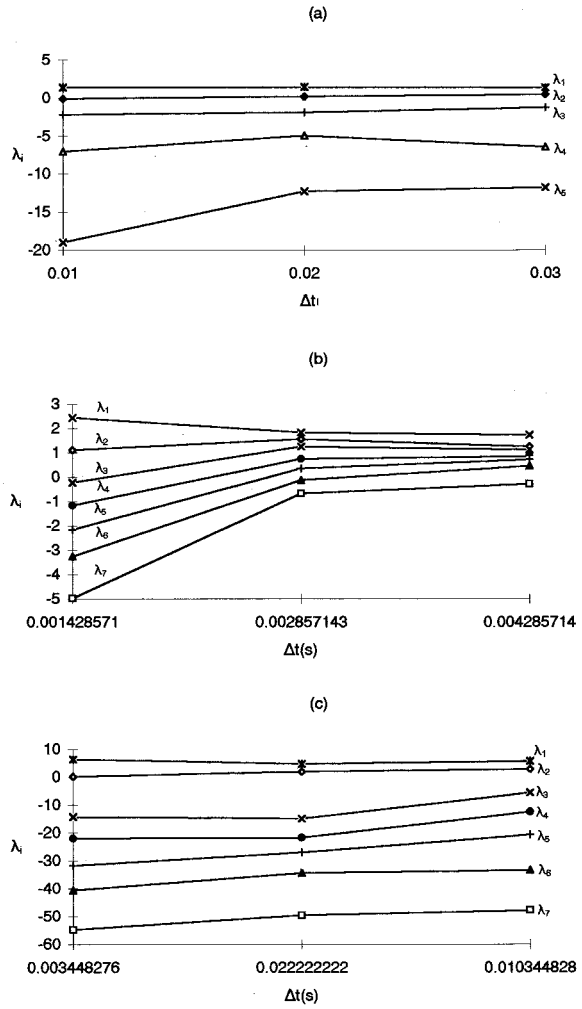

FIG. 11. The effect of the sampling rate Δt^{-1} on the results of the Eckmann *et al.* algorithm. (a) Effect of Δt^{-1} on the Lyapunov spectrum of the Lorenz signal; (b) effect of Δt^{-1} on Signal 1, and (c) effect of Δt^{-1} on Signal 2.

VI. STUDY OF THE RECONSTRUCTION PARAMETERS m,τ

A. The effect of the embedding dimension m

The reconstruction of the attractor from a scalar time series is based on a theorem proved by Takens [1]:

If $y:M\rightarrow\mathbb{R}$ is an observable smooth function, M is a compact manifold of dimension d, $\varphi_t(\mathbf{x})$ is the time evolution of the dynamical system and $\mathbf{x}$ is a smooth vector field then the map: $M\rightarrow\mathbb{R}^{2d+1}$, defined by,

$$\mathbf{\Phi}(\mathbf{x})=[y(\mathbf{x}),y(\varphi(\mathbf{x})),\ldots,y(\varphi_{2d}(\mathbf{x}))] \tag{50}$$

is an embedding.

The above theorem states that the sufficient, but not necessary, condition for an attractor of a dynamical system of dimension d to be embedded in an m-dimensional space is $m\geqslant 2d+1$. The dimension of the space in which the attractor is reconstructed is called the embedding dimension. The theorem can be applied directly in the case of the scalar time series to obtain Eq. (26). If the dimension d of the system is known or is guessed by intuition then a sufficiently large embedding dimension m can be used in order to fulfil the condition of the above theorem.

As can be seen from Eqs. (31) and (34) the Lyapunov spectrum consists of m exponents, equal to the embedding dimension m. Hence if the embedding dimension is chosen to be greater than the minimum required embedding dimension then some spurious exponents will be calculated among the true ones.

The minimum m can be calculated directly by several techniques and thus the true Lyapunov spectrum can be obtained [31,32]. Additionally, the time-reversal method proposed by Parliz can be possibly used to determine all spurious exponents [33]. An empirical approach is to reveal the spurious Lyapunov exponents from their m dependence. Fortunately, in many cases the spurious exponents lie between the most negative exponent and zero and tend to wonder with m. In these cases, if we are interested solely in the value of the positive exponent(s) the spurious (negative) exponents do not cause any confusion. The appearance of the spurious Lyapunov exponents, which are about twice the true ones, is very often. This phenomenon is generated by the finiteness of the scalar time series where one expects nonlinearities to be important, as in the case of the Hénon map [11] or even the Lorenz equations (see below). If the noise of the system is not too small relative to the precision and the density of the data, one will see the true Lyapunov exponents and the spurious ones will all be negative.

The procedure for the study of the m dependence of the spectrum is the same as in the preceding sections where the constant values of the rest of the parameters are presented in Table I. The effect of m on the calculated values of the Lyapunov exponents of the Lorenz signal using the Sano and Sawada algorithm is shown in Fig. 12(a). As can be seen for $m=3$ the three real exponents are calculated. For $m=4$ a spurious exponent emerges which is negative. For $m=5$ two spurious exponents exist, a negative one and a positive which is twice the largest true exponents. For $m=6$ a third spurious exponent is revealed which has a positive value, thrice the largest true exponent. For $m=7$ another spurious exponent is born which is negative.

In Fig. 12(b) we observe the dependence of the Lyapunov spectrum on the embedding dimension for Signal 1. For $m=3$ the three Lyapunov exponents are present. By increasing m another negative exponent is born. For $m=5$ the most negative exponent is also calculated. For $m=6$ a new exponent is present which is negative. Finally, for $m=7$ a second positive exponent is born which is smaller than the most positive Lyapunov exponent. As can be seen in Fig. 12(b) no positive spurious exponents are present with values greater than the largest true exponent, no matter how large m is chosen.

A somehow similar effect is observed for Signal 2 in Fig. 12(c). Thus for $m=3$ three exponents are calculated where the positive and the zero one remain fairly constant by increasing m. For $m=4$ a new negative exponent is calculated. For $m=5$ another negative exponent is born, as well as for $m=6$ and $m=7$ where all new exponents are negative. Once again, no positive spurious exponents are present with values greater than the largest true exponent, no matter how large m is chosen.

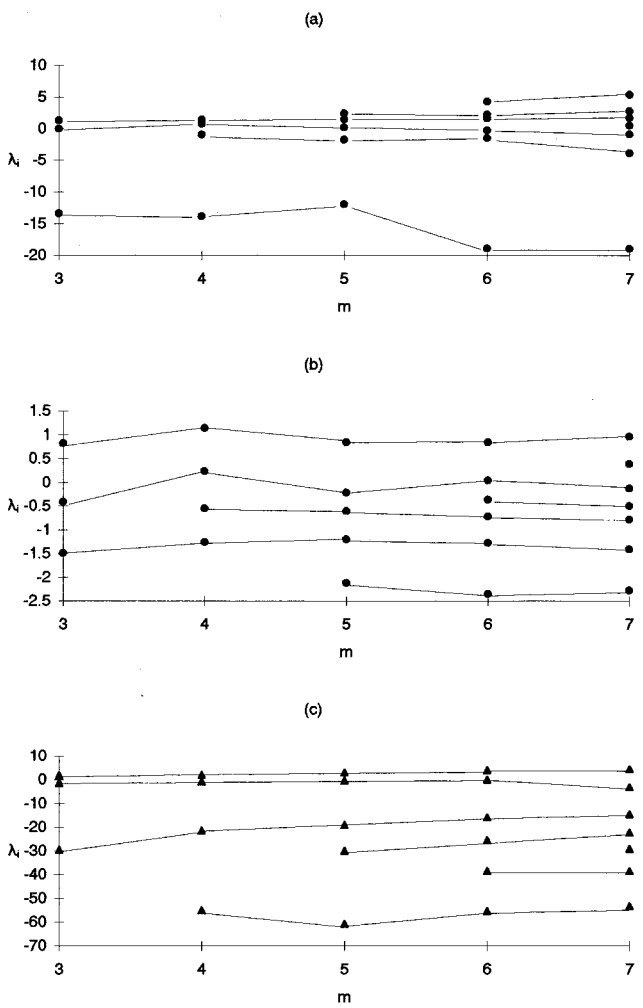

FIG. 12. The effect of the embedding dimension m on the results of the Sano and Sawada algorithm. (a) Effect of m on the Lyapunov spectrum of the Lorenz signal; (b) effect of m on Signal 1, and (c) effect of m on Signal 2.

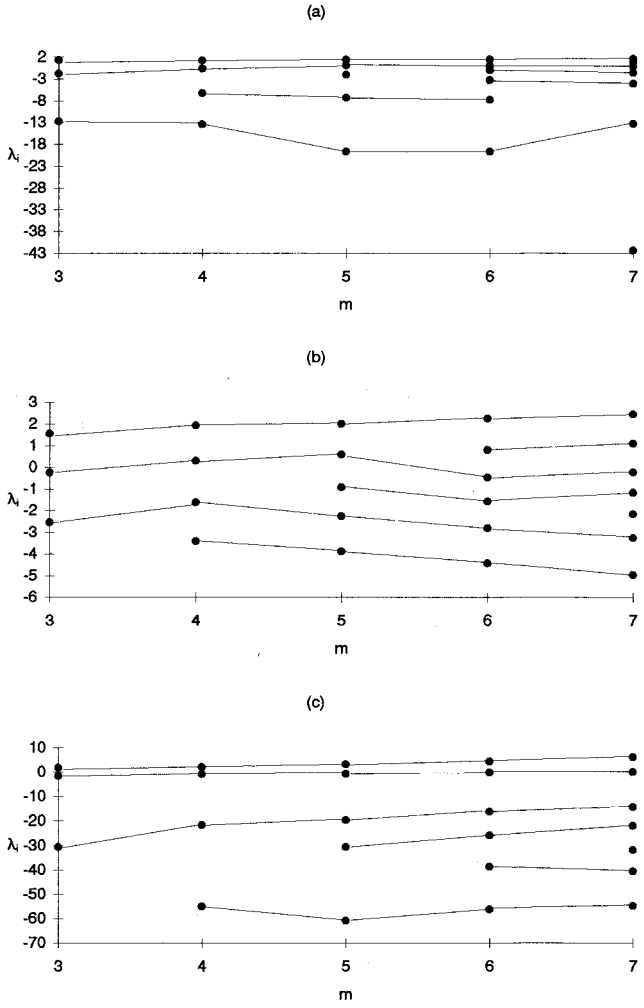

FIG. 13. The effect of the embedding dimension m on the results of the Eckmann *et al.* algorithm. (a) Effect of m on the Lyapunov spectrum of the Lorenz signal; (b) effect of m on Signal 1, and (c) effect of m on Signal 2.

The trend of the spectrum of the Lorenz signal by varying m when the Eckmann *et al.* algorithm is used is presented in Fig. 13(a). It is obvious that the birth of a spurious positive exponent does not place no matter how large m becomes. For $m=3$, the three exponents are calculated which, all of them, deviate from the real values. For $m=4$ a new exponent is born which is negative. For $m=5$ another negative exponent is calculated and the three true exponents tend to the theoretical values. For $m=6$ a third negative exponent is calculated. For $m=7$ the picture changes drastically with the birth of a positive exponent which is smaller that the positive true exponent and a negative exponent with a very large absolute value. The true negative exponent also shifts to lower absolute values for $m=7$.

The effect of the choice m on the Lyapunov spectrum of Signal 1, by using the Eckmann *et al.* algorithm is presented in Fig. 13(b). It is obvious that no spurious exponents greater than the true positive exponent are present. By increasing m from 3 to 5 only negative exponents are revealed. For $m=6$ a positive exponent is born with a value smaller that the true positive one. For $m=7$ an additional negative exponent is calculated. A similar shift takes place in the case of the calculation of the Lyapunov spectrum of Signal 2 with the use of the Eckmann *et al.* algorithm. In Fig. 13(c) the exponents are born regularly by increasing m and are all negative.

B. The effect of the time delay $\tau\Delta t$

For the application of the Takens' theorem Eq. (26) requires the input of a time delay for the construction of the m-dimensional vectors which consist of the reconstructed attractor. For an infinite amount of high precision data points, i.e., a noiseless scalar time series of infinite duration, the time delay can be chosen arbitrarily. In the case of the physical experiments there is of course a lower limit for the choice of the time delay which is equal to the sampling time Δt. For a very small time delay $\tau\Delta t \to 0$, all the reconstructed vectors will be highly correlated and the attractor will lie on a straight line. By increasing τ the reconstructed vectors become more uncorrelated and the reconstruction will capture the geometry and the statistical properties of the underlying system.

A naive selection of τ is the value for which the autocorrelation function first passes through zero. If the autocorre-

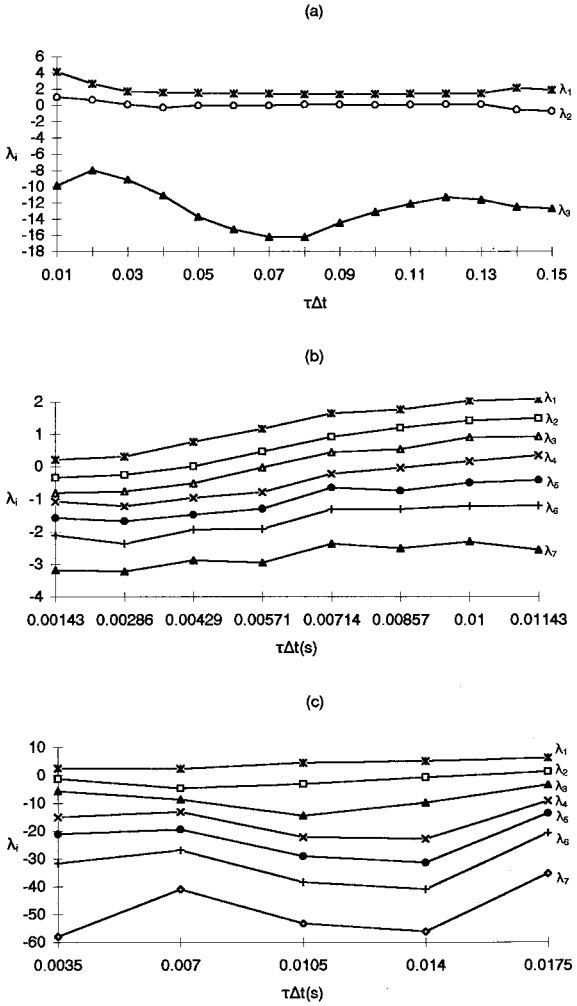

FIG. 14. The effect of the time delay τ on the results of the Sano and Sawada algorithm. (a) Effect of τ on the Lyapunov spectrum of the Lorenz signal; (b) effect of τ on Signal 1, and (c) effect of τ on Signal 2.

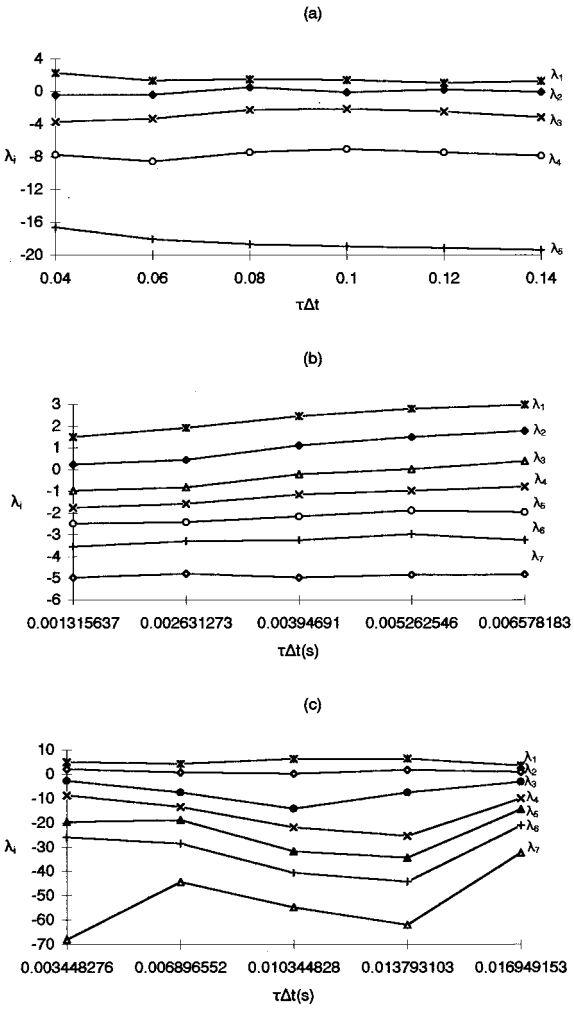

FIG. 15. The effect of the time delay τ on the results of the Eckmann *et al.* algorithm. (a) Effect of τ on the Lyapunov spectrum of the Lorenz signal; (b) effect of τ on Signal 1, and (c) effect of τ on Signal 2.

lation function does not pass through zero, its first minimum can also be used as a proper time delay. As pointed out by Fraser and Swinney [34], the autocorrelation function expresses linear independence and thus the above choice of the time delay is actually gross. The same authors as well as Liebert and Schuster [35] propose that the proper choice of the time delay is the value which corresponds to the first minimum of the mutual information which expresses general dependence of the variables.

In order to study the effect of τ on both algorithms, we vary the time delay $\tau\Delta t$ for fixed values of the rest of the parameters (Table I). When the Sano and Sawada algorithm is implemented, the Lyapunov spectrum actually depends on the choice of the time delay $\tau\Delta t$ as can be seen in Fig. 14(a). For $\tau\Delta t<0.05$ the calculated values of the Lyapunov exponents deviate from the theoretically calculated values. At the region $0.05\leqslant\tau\Delta t\leqslant0.1$ the Lyapunov spectrum is very close to the true value. We must notice that this region is very close to the region where the autocorrelation function of the Lorenz signal passes through zero.

The effect of the choice of τ on the spectrum of Signal 1 is shown in Fig. 14(b). It is obvious that the calculated values depend on the choice of the time delay. We can say that the more suitable choice of $\tau\Delta t$ is the value 0.0043 sec where the exponent λ_2 takes a value close to zero ($3.46\ 10^{-3}$). For all the other values of $\tau\Delta t$, a large deviation of the zero exponent is observed.

More stable results are obtained when the Sano and Sawada algorithm is used for the determination of the Lyapunov spectrum of Signal 2, for various values of $\tau\Delta t$. The dependence of the Lyapunov exponents on the time delay is presented in Fig. 14(c) where a choice of the time delay in the region 0.007 sec$<\tau\Delta t<$0.0175 sec seems to give stable and reasonable values of the Lyapunov exponents.

The effect of $\tau\Delta t$ in the calculation of the Lyapunov exponents of the Lorenz signal by using the Eckmann *et al.* algorithm is presented in Fig. 15(a). As it can be seen from this figure for $\tau\Delta t\geqslant0.028$ the spectrum is constant and does not depend strongly on the choice of the time delay.

The trend of the spectrum by varying $\tau\Delta t$ when the Eckmann *et al.* algorithm in used for Signal 1 is shown in Fig. 15(b). As it can be seen, for $\tau\Delta t>0.0026$ sec no zero exponent is observed and a shift of the spectrum to higher values

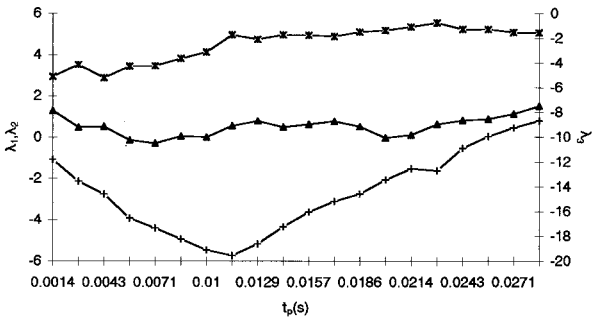

FIG. 16. The use of the Gramm-Schmidt orthonormalization instead of the Householder transformations in the Eckmann *et al.* algorithm. A direct comparison with Fig. 7(a) gives an indication of the poor accuracy of the calculations.

is observed. Thus a suitable choice of the time delay should be $\tau\Delta t \leqslant 0.0026$ sec.

By inspecting Fig. 15(c) we observe that the time delay has an effect on the calculation of the Lyapunov exponents of Signal 2. Only for time delay values in the interval $0.003 \text{ sec} < \tau\Delta t < 0.014$ sec a zero exponent is calculated and thus, these values can be considered as suitable for the proper choice of $\tau\Delta t$.

VII. DISCUSSION OF THE RESULTS

In the present work we presented a brief description of the Sano and Sawada and Eckmann *et al.* algorithms for the calculation of the Lyapunov spectrum from experimental signals and we compared analytically and numerically the two algorithms. We used a uniform formulation of the algorithms which allowed us to prove that the calculated value of the largest exponent is identical for both algorithms but there is a mismatch of the rest of the spectrum. The above result was confirmed with numerical calculations of the Lyapunov spectrum for one time series obtained from the Lorenz equations and two time series obtained experimentally from the electrochemical system $Fe-2M H_2SO_4$.

The calculation of the Lyapunov spectrum by using the Sano and Sawada or the Eckmann *et al.* algorithm is based on some assumptions which introduce a number of ambiguities for the implementation of the algorithms. It is always assumed that the operator $\mathbf{Df}(\mathbf{x})$ is a continuous function in the region defined by the propagation time, even for every stiff experimental signals like the one presented in Fig. 1(b). The general solution of Eq. (11) is expected to have the form of Eq. (12) in the region of continuity of the operator $\mathbf{Df}(\mathbf{x})$. It is obvious that this assumption is difficult to be verified numerically.

Another assumption which cannot be verified is that the radius ε of the small sphere is considered as infinitesimally small. It is well known that we expect the divergence of nearby orbits to be exponential, if these are initially separated only infinitesimally. Although, very often ε is taken to be quite large in order to avoid interference of the noise of the system.

The linearity of Eq. (29) is another crucial assumption. The use of linear least squares assumes that the vectors $\mathbf{z}_j$ are related linearly with the vectors $\mathbf{y}_j$ (as was originally suggested [11,12]). This assumption is supposed to be valid if the small propagation time is used. Nevertheless the choice of t_p is not straightforward and in the case of stiff signals with small peak-to-peak time intervals it must be chosen rather large due to the small value of the sampling rate. Additionally, we must point out that even though the Lyapunov exponents are defined for $t \to \infty$, both algorithms do not calculate the spectrum for asymptotic time but they rather measure the mean exponential divergence in the time scale of the propagation time for k times ($k \to \infty$).

Even though the validity of the above restrictions cannot be proven rigorously, numerical experiments often suggest that assumptions actually hold to some degree. In the present work, we apply both algorithms for the calculation of the Lyapunov exponents of the Lorenz signal Eq. (9). They were found to be very close to those values calculated from the variational equations Eq. (13). The same can be assumed to hold for the smooth signals, like Signal 2. On the other hand, the results concerning extreme situations (like Signal 1) must be interpreted very thoughtfully.

The Sano and Sawada and the Eckmann *et al.* algorithms were compared numerically for six parameters, namely, the radius of the sphere, the propagation time, the maximum number of points, the sampling rate, the embedding dimension, and the time delay, for three different time series. The comparison showed that the Eckmann *et al.* algorithms is more independent of the choice of ε than the Sano and Sawada algorithm, for the noise-free signal obtained from the Lorenz equations. The same conclusion can be drawn for the smooth experimental Signal 2; the Eckmann *et al.* algorithm shows a plateau of some extent bigger than the one of the Sano and Sawada algorithm and it calculates more accurately the zero exponent. Both algorithms deviate from the true values of the exponents for small values of ε in the case of the noisy experimental signals. In order to avoid small choices of ε a shell rather than a sphere can be used for the formation of the small vectors $\mathbf{y}_j$ [22]. A similar effect is not observed on the noise-free Lorenz signal, where the best results are obtain for small ε. The linear approximation of the operator $\mathbf{A}(t)$ is expected to be accurate if ε is selected as described above, even though a nonlinear approximation would improve the determination of $\mathbf{A}(t)$ [17,18].

The second algorithm parameter the propagation time t_p has a strong effect on the Lyapunov spectrum for both algorithms. In order to utilize the linear-least-squares approximation of $\mathbf{A}(t)$, t_p must not be large. On the other hand, extremely small propagation time will lead to the false calculation of the unreasonably large Lyapunov exponents. This effect is observed for both algorithms, especially when the Lyapunov spectrum of the stiff Signal 1 is calculated. The situation can be less dramatic if the smaller sampling rate is used, where this is permissible. In the case of the smooth Signal 2, where the sampling rate is four times less of the sampling rate of Signal 1, smaller propagation time can be used and a larger plateau region can be located. Unfortunately, a smaller sampling rate cannot be used for the stiff signals which contain sharp peaks with small peak-to-peak time intervals because the choice of a smaller sampling rate will cause a bad quality signal from which any calcula-

tion would be nonsense. We expect results of poor accuracy, from both algorithms, when a very stiff signal is recorded, which is necessary with a large sampling rate. From the results we may conclude that the propagation time is proportional to the dominant frequency of the aperiodic signal.

In this point we must notice that the accuracy of the results depends also on the numerical techniques used by the algorithms. The Sano and Sawada algorithm seems to be independent of the type of the orthonormalization used, that is, the utilization of the Gramm-Schmidt or the Householder transformation procedure. In contrast, the results of the Eckmann *et al.* algorithm depend strongly on the choice of the orthonormalization procedure. In principal, both algorithms utilize an orthonormalization procedure; the Sano and Sawada algorithm in order to orthonormalize the vectors $\mathbf{e}_i^{(j)}$ and the Eckmann *et al.* algorithm in order to construct the orthogonal matrix $\mathbf{Q}_i$. For all the results presented in Secs. IV, V, and VI, as far as it concerns the Eckmann *et al.* algorithm, the Householder transformation was used. For the sake of comparison in Fig. 16 we present the same calculations as the ones presented in Fig. 7(a), by using the Gramm-Schmidt orthonormalization procedure. It is obvious that the Eckmann *et al.* algorithm gives very inaccurate results when this orthonormalization procedure is used.

Even though a very large number of data points is assumed to be required in order to calculate the Lyapunov spectrum, by decreasing the number of points for smooth signals the Lyapunov spectrum remains fairly constant even for values less than 10 000 points. In contrast, the Lyapunov spectrum of stiff signals seems more sensitive to the decrease of $N_{\max}$. Thus, only for $N_{\max} \geqslant 80\,000$ points, the Lyapunov spectrum seems to converge to the true values.

The number of data points $N_{\max}$ must be large by means of the maximum possible total sampling time and not due to a large sampling rate Δt^{-1}. In the case of a smooth signal the sampling rate must have a moderate value; not too small in order for the small vectors $\mathbf{y}_j$ to lie in different orbits and not too large in order to capture all the features of the system. This rule is difficult to apply in the case of the stiff signals. Stiff signals have to be recorded with a very small sampling rate Δt^{-1} and thus the Lyapunov spectrum is suspected to be overestimated or even inaccurate, indifferently of the algorithm used.

It must be pointed out that the Eckmann *et al.* algorithm is more sensitive to the selection of m. For small m the accuracy of the results is rather poor and a larger embedding dimension is necessary. On the other hand, the Sano and Sawada algorithm converges even for small m. The birth of spurious exponents occurs for both algorithms.

A great deal of the literature is devoted to the existence of spurious exponents among the true ones when a calculation is done directly from the time series [19,31,32]. Some techniques are already proposed either for the calculation of the minimum embedding dimension or for the direct determination of spurious exponents [5,33]. Fortunately, spurious exponents often have values between the zero exponent and the most negative one. It is possible that positive spurious exponents which are twice or thrice that of the real positive exponent will be born for increasing values of m. We must notice that when the signal is not noise free the birth of double or triple exponents does not take place. In this case all spurious exponents lie between the largest and the smallest exponent and so the signal can be characterized safely.

Even though in principle the time delay τ can be chosen arbitrarily, its choice is very crucial when dealing with experimental signals of finite duration and low precision. The value of τ can be chosen somehow empirically by varying its value and searching for a plateau at the spectrum, a zero exponent and a negative divergence of the vector field. In the case of the Lorenz signal, the proper τ determined by this way is very close to the first zero crossing of the autocorrelation function.

We should notice the large difference of the values of the Lyapunov exponents of the two experimental signals by varying the bifurcation parameters R (ohmic resistance) and E (applied potential). This is due to the fact that the Lyapunov exponents are discontinuous functions of the bifurcation parameters and thus we do not expect a continuous variation of the values of the exponents by varying the bifurcation parameters [4].

We observe that the Eckmann *et al.* algorithm better approximates the zero and negative exponents in most cases and it seems more promising for the accurate determination of the whole spectrum. In general, the Eckmann *et al.* algorithm gives stable Lyapunov exponents for a larger region of the parameters and thus more easily determines the Lyapunov spectrum. Its sensitivity to the choice of the orthonormalization procedure and the requirement of a large embedding dimension is balanced by the more accurate determination of the Lyapunov spectrum. On the other hand, the Sano and Sawada algorithm is easy to implement and can determine the Lyapunov exponents for smaller values of the embedding dimension.

As a conclusion we may say that even though the central idea of the Sano and Sawada and the Eckmann *et al.* algorithms is the same, the later is superior due to the numerical methodology used and it can determine the whole spectrum more accurately. If we are interested only for the characterization of the nonlinear time series, any of the two algorithms can be used to calculate the largest Lyapunov exponent. The calculated Lyapunov exponents strongly depend on the algorithm, signal and reconstruction parameters and the results are expected to be accurate only in a parameter region, often narrow, which must be chosen carefully by trying to fulfill the basic assumptions and performing a variety of numerical experiments. The stiffness of the signal is of a great importance and results concerning this kind of signals must be interpreted thoughtfully.

Future work on the determination of the Lyapunov spectrum from experimental signals must aim not only to the improvement of the accuracy of the numerical techniques and procedures of the algorithms but also to the introduction of quantitative criteria which will allow an easy, proper, and even *a priori* choice of the six algorithm parameters. A convenient choice of the algorithm parameters will permit the use of the two algorithms as common scientific tools for the characterization and study of nonlinear experimental signals.

ACKNOWLEDGMENT

This work was partially supported under P.E.N.E.D. 91/ED/780 of the Greek General Secretariat of Research and Technology.

[1] F. Takens, *Dynamical Systems and Turbulence, Warwick, 1980*, Lecture Notes in Mathematics, edited by D. Rand and L. S. Young (Springer, Berlin, 1981), Vol. 898, p. 366.
[2] D. Ruelle, *Bifurcation Theory and Applications in Scientific Disciplines*, edited by O. Gurel and O. E. Rossler (New York Academy of Sciences, New York, 1979) p. 316.
[3] D. Kahaner, C. Moler, and S. Nasy, *Numerical Methods and Software*, in Computational Mathematics (Prentice-Hall, Englewood Cliffs, NJ, 1989).
[4] J.-P. Eckmann and D. Ruelle, Rev. Mod. Phys. **57**, 617 (1985).
[5] D. Ruelle, *Chaotic Evolution and Strange Attractors* (Cambridge University Press, Cambridge, 1989), pp. 45–61.
[6] P. Grassberger and I. Procaccia, Phys. Rev. Lett. **50**, 346 (1983).
[7] Y. B. Pesin, Russ. Math. Surv. **32**, (4), 55 (1977).
[8] P. Frederickson, J. L. Kaplan, E. D. Yorke, and J. A. Yorke, J. Diff. Eq. **49**, 185 (1983).
[9] L.-S. Young, Physica A **124**, 639 (1984).
[10] A. Wolf, J. B. Swift, H. L. Swinney, and J. A. Vastano, Physica D **16**, 285 (1985).
[11] J.-P. Eckmann, S. O. Kamphorst, D. Ruelle, and S. Cilibert, Phys. Rev. A **34**, 4971 (1986).
[12] M. Sano and Y. Sawada, Phys. Rev. Lett. **55**, 1082 (1985).
[13] H. Kantz, Phys. Lett. A **185**, 77 (1994).
[14] H. Haken, Phys. Lett. A **94**, 71 (1983).
[15] H. D. Abarbanel, Rev. Mod. Phys. **65**, 1331 (1993).
[16] H. D. Abarbanel, R. Brown, and M. B. Kennel, J. Nonlinear Sci. **2**, 343 (1992).
[17] K. Briggs, Phys. Lett. A **151**, 27 (1990).
[18] P. Bryant, R. Brown, and H. D. Abarbanel, Phys. Rev. A **43**, 2787 (1990).
[19] W. Huang, W. X. Ding, D. L. Feng, and C. X. Yu, Phys. Rev. E **50**, 1062 (1994).
[20] R. Stoop and P. F. Meier, J. Opt. Soc. Am. B **5**, 1037 (1988).
[21] R. Stoop and J. Parisi, Physica D **50**, 89 (1991).
[22] X. Zeng, R. Eykholt, and R. A. Pielke, Phys. Rev. Lett. **66**, 3229 (1991).
[23] Th.-M. Kruel, M. Eiswirth, and F. W. Schneider, Physica D **63**, 117 (1993).
[24] J. B. Katdtke, J. Brush, and J. Holzfuss. Int. J. Bifurc. Chaos **3**, 607 (1993).
[25] D. Sazou, A. Karantonis, and M. Pagitsas, Int. J. Bifurc. Chaos **3**, 981 (1993).
[26] E. A. Coddington and N. Levinson, *Theory of Ordinary Differential Equations* (McGraw-Hill, New York, 1955), pp. 11–13, 67–81.
[27] V. I. Oseledec, Trans. Moscow Math. Soc. **19**, 197 (1968).
[28] I. Goldhirsch, P.-L. Sulem, and S. A. Orszag, Physica D **27**, 311 (1987).
[29] J. H. Wilkinson, *The Algebraic Eigenvalue Problem* (Clarendon, Oxford, 1965), pp. 485–524, 602–609.
[30] J.-P. Eckmann and D. Ruelle, Physical D **56**, 185 (1992).
[31] D. S. Broomhead and G. P. King, *Nonlinear Phenomena and Chaos*, edited by S. Sarkar (Hilger, Bristol, 1986), p. 113.
[32] M. B. Kennel, R. Brown, and H. D. I. Abarbanel, Phys. Rev. A **45**, 3403 (1992).
[33] U. Parlitz, Int. J. Bifurc. Chaos **2**, 155 (1992).
[34] A. M. Fraser and H. L. Swinney, Phys. Rev. A **33**, 1134 (1986).
[35] W. Liebert and H. G. Schuster, Phys. Lett. A **142**, 107 (1989).